

Ivan Vitev

Overview of inclusive light hadron and jet suppression observables at RHIC and the LHC

High p_T in the RHIC-LHC Era, April 2016

Brookhaven National Laboratory, Upton, NY

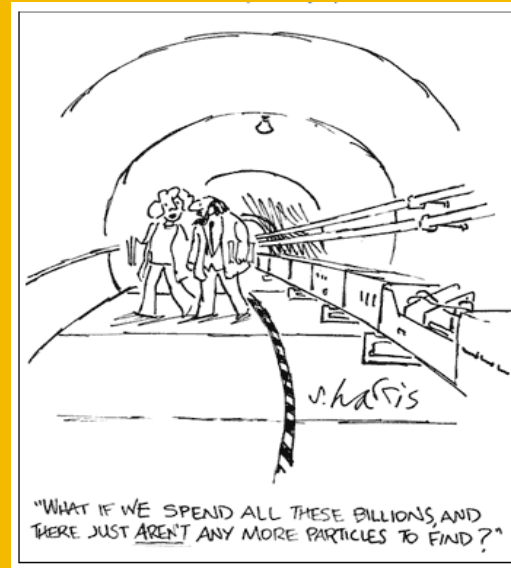
Outline of the talk

Thanks to the organizers for the invitation

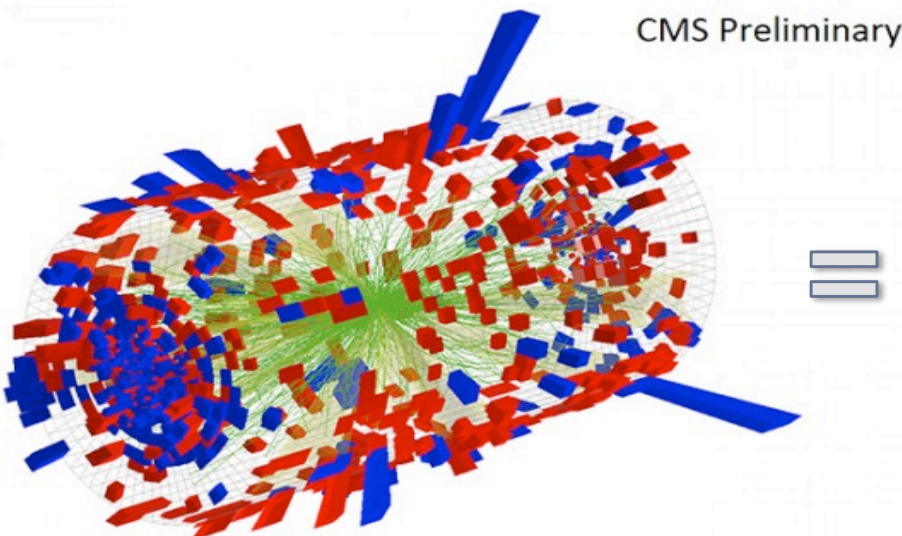
Work done in collaboration with *Y.T. Chien, W. Dai, A. Emerman, J. Huang, Z. Kang, R. Lashof-Regas, B. Neufeld, G. Ovanesyan, F. Ringer, P. Saad, H. Xing, B.W. Zhang*

- An effective theory for jet propagation in matter SCET_G. A tool to improve upon the energy loss approach. Medium induced splitting kernels
- Connecting the energy loss and the QCD evolution approaches. Illustration at RHIC. LHC phenomenology and predictions
- Evolution and resummation for jet substructure observables and jet shapes. NLL results in p+p collisions
- Quenching of reconstructed jets, modification of the differential jet shapes beyond the energy loss approach
- Photon-tagged jets, momentum imbalance, and photon tagged jet shapes
- Other new topics in perturbative jet quenching theory

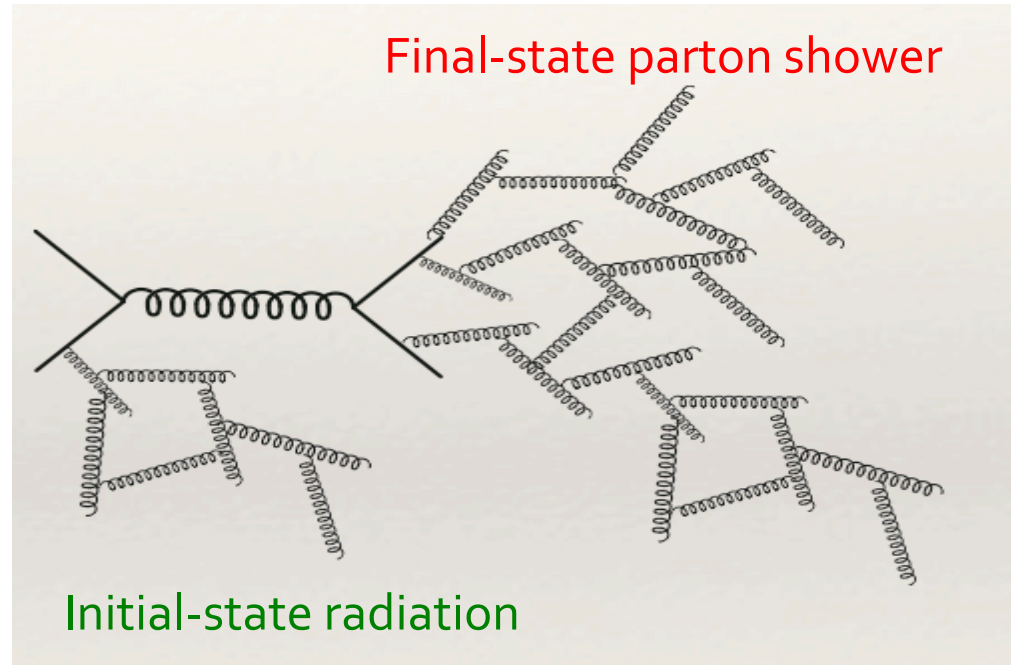
I. Background and theoretical preliminaries



Logs, Legs, and Loops



S. Chatrchyan et al. PLB (2013)



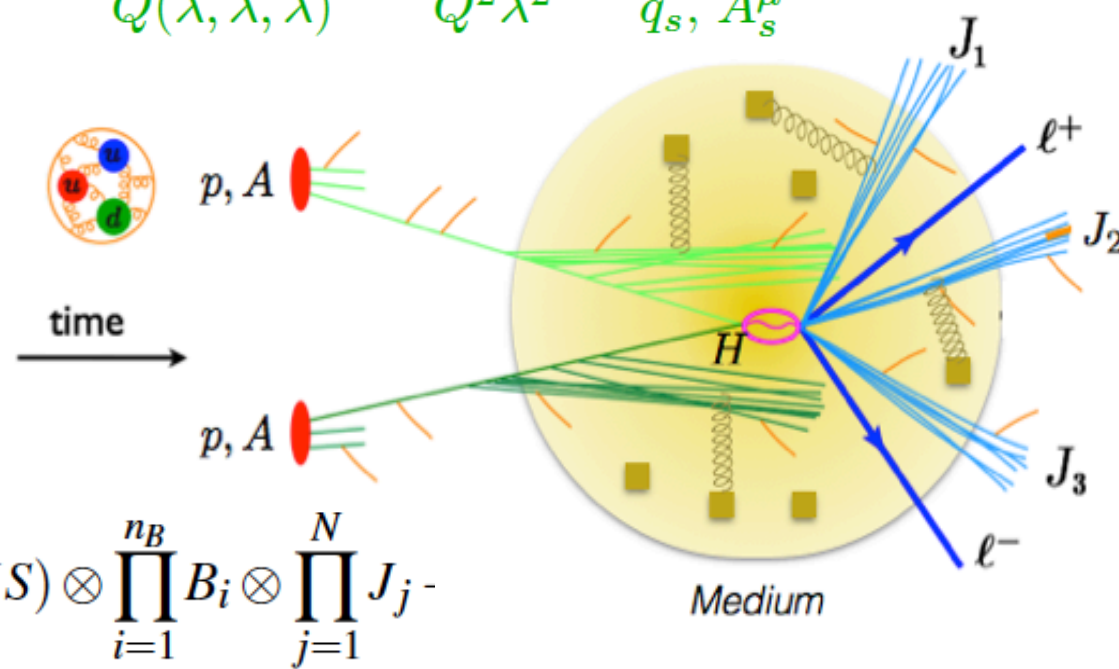
- Traditional energy loss approach, phenomenologically successful but cannot be systematically improved, higher orders and resummation
- In HEP significant effort has been devoted to understanding the parton shower. We demonstrate how this parton shower technology can be applied to heavy ion reactions, NLO, NLL, etc
- The same techniques should be applied to hard probes: particles, jets, and heavy flavor

The big picture

- Jet physics presents a multiscale problem, EFT treatment

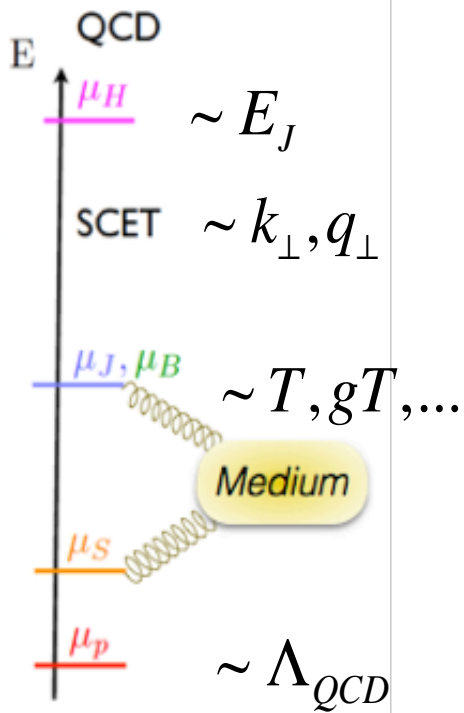
SCET (Soft Collinear Effective Theory)

| modes | $p^\mu = (+, -, \perp)$ | p^2 | fields |
|-----------|--------------------------------|-----------------|------------------|
| collinear | $Q(\lambda^2, 1, \lambda)$ | $Q^2 \lambda^2$ | ξ_n, A_n^μ |
| soft | $Q(\lambda, \lambda, \lambda)$ | $Q^2 \lambda^2$ | q_s, A_s^μ |



C. Bauer et al. (2001)

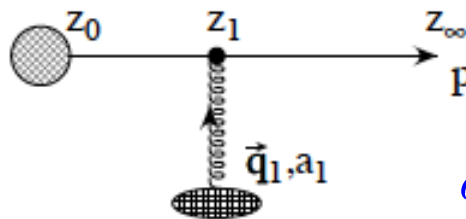
D. Piran et al. (2004)



- Factorization theorems written in terms of Jet (J), beam (B), and soft (S) functions

Soft collinear effective theory with Glauber Gluons - SCET_G

- Jet (and heavy flavor production) production in the medium remains a multi-scale problem



Glauber gluons to mediate physical interactions with the QCD medium

$$q = (\lambda^2, \lambda^2, \lambda)Q$$

A. Idilbi et al. (2008)

Ovanesyan et al. (2011)

- Background field approach. Factorization, with modified J, B, S. Feynman rules derived for different sources and gauges

$$\mathcal{L}_G(\xi_n, A_n, \eta) = \sum_{p, p', q} e^{-i(p-p'+q)x} \left(\bar{\xi}_{n,p'} \Gamma_{qqA_G}^{\mu,a} \frac{\bar{\eta}}{2} \xi_{n,p} - i \Gamma_{ggA_G}^{\mu\nu\lambda,abc} (A_{n,p'}^c)_\lambda (A_{n,p}^b)_\nu \right) \bar{\eta} \Gamma_s^{\delta,a} \eta \Delta_{\mu\delta}(q)$$

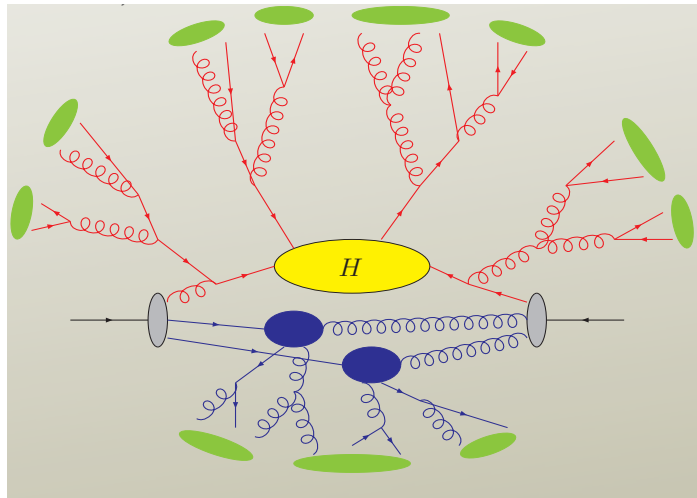
- Also operator approach with focus on small-x physics

S. Fleming, (2014)

I. Rothstein et al, (2016)

Effective potential,
e.g. Gyulassy-Wang

In-medium parton splittings, properties, and DGLAP evolution



G. Altarelli et al. (1977)

- Implemented in DGLAP evolution equations

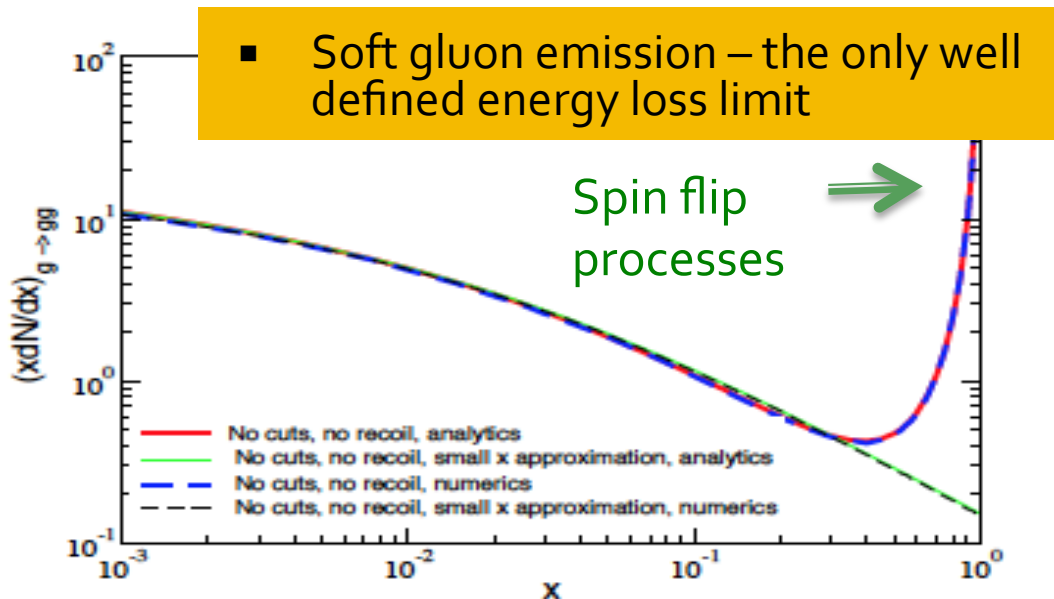
$$\frac{dN(\text{tot.})}{dx d^2 k_\perp} = \frac{dN(\text{vac.})}{dx d^2 k_\perp} + \frac{dN(\text{med.})}{dx d^2 k_\perp}$$

G. Ovanesyan et al. (2012)

$$\left(\frac{dN}{dx d^2 k_\perp} \right)_{q \rightarrow qg} = \frac{\alpha_s}{2\pi^2} C_F \frac{1 + (1-x)^2}{x} \int \frac{d\Delta z}{\lambda_g(z)} \int d^2 q_\perp \frac{1}{\sigma_{el}} \frac{d\sigma_{el}^{\text{medium}}}{d^2 q_\perp} \left[- \left(\frac{A_\perp}{A_\perp^2} \right)^2 + \frac{B_\perp}{B_\perp^2} \cdot \left(\frac{B_\perp}{B_\perp^2} - \frac{C_\perp}{C_\perp^2} \right) \right. \\ \times (1 - \cos[(\Omega_1 - \Omega_2)\Delta z]) + \frac{C_\perp}{C_\perp^2} \cdot \left(2 \frac{C_\perp}{C_\perp^2} - \frac{A_\perp}{A_\perp^2} - \frac{B_\perp}{B_\perp^2} \right) (1 - \cos[(\Omega_1 - \Omega_3)\Delta z]) \\ + \frac{B_\perp}{B_\perp^2} \cdot \frac{C_\perp}{C_\perp^2} (1 - \cos[(\Omega_2 - \Omega_3)\Delta z]) + \frac{A_\perp}{A_\perp^2} \cdot \left(\frac{A_\perp}{A_\perp^2} - \frac{D_\perp}{D_\perp^2} \right) \cos[\Omega_4 \Delta z] \\ \left. + \frac{A_\perp}{A_\perp^2} \cdot \frac{D_\perp}{D_\perp^2} \cos[\Omega_5 \Delta z] + \frac{1}{N_c^2} \frac{B_\perp}{B_\perp^2} \cdot \left(\frac{A_\perp}{A_\perp^2} - \frac{B_\perp}{B_\perp^2} \right) (1 - \cos[(\Omega_1 - \Omega_2)\Delta z]) \right].$$

N.B. $x \rightarrow 1-x$ $A, \dots, D, \Omega_1 \dots \Omega_5$ – functions(x, k_\perp, q_\perp)

As in vacuum, a total of 4 splitting functions



QCD evolution in the soft gluon energy loss limit

$$\frac{df_q(x, Q)}{d \ln Q} = P_{q \rightarrow qg} \otimes f_q + P_{g \rightarrow q\bar{q}} \otimes f_g$$

$$\frac{df_g(x, Q)}{d \ln Q} = P_{g \rightarrow gg} \otimes f_g + \sum_{q, \bar{q}} P_{q \rightarrow gq(\bar{q})} \otimes f_q$$

$$P_{q \rightarrow qg} = \frac{2C_F}{x_+} + \left(\frac{2C_F}{x} g[x, Q, L, \mu] \right)_+,$$

$$P_{g \rightarrow gg} = \frac{2C_A}{x_+} + \left(\frac{2C_A}{x} g[x, Q, L, \mu] \right)_+,$$

$$P_{g \rightarrow q\bar{q}} = 0, \quad P_{q \rightarrow gq} = 0,$$

- If a connection is to be found between the energy loss and the evolution approach, it is in the soft gluon limit
- We solve the DGLAP evolution equations analytically

$$D_{h/c}^{\text{med.}}(z, Q) = e^{-2C_R \frac{\alpha_s}{\pi} \left[\ln \frac{Q}{Q_0} \right] \{ [n(z)-1](1-z) - \ln(1-z) \}} D_{h/c}(z, Q_0)$$

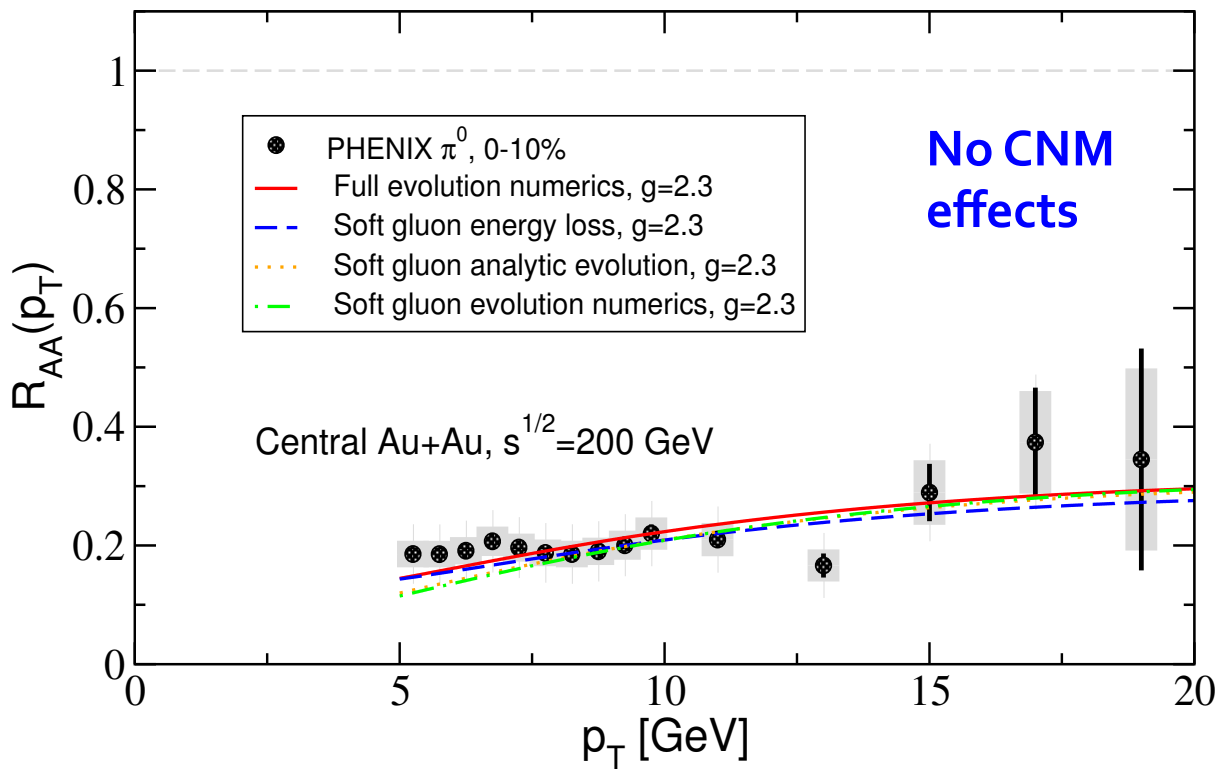
Analytic solution to DGLAP evolution

$$\begin{aligned} & \times e^{-[n(z)-1] \left\{ \int_0^{1-z} dz' z' \int_{Q_0}^Q dQ' \frac{dN}{dz' dQ'}(z', Q') \right\} - \int_{1-z}^1 dz' \int_{Q_0}^Q dQ' \frac{dN}{dz' dQ'}(z', Q')} \\ & = D_{h/c}(z, Q) e^{-[n(z)-1] \langle \frac{\Delta \tilde{E}}{E} \rangle_z - \langle N^g \rangle_z}. \end{aligned}$$

- *The main result:* direct relation between the evolution and energy loss approaches first established here

Comparison of energy loss and QCD evolution approaches

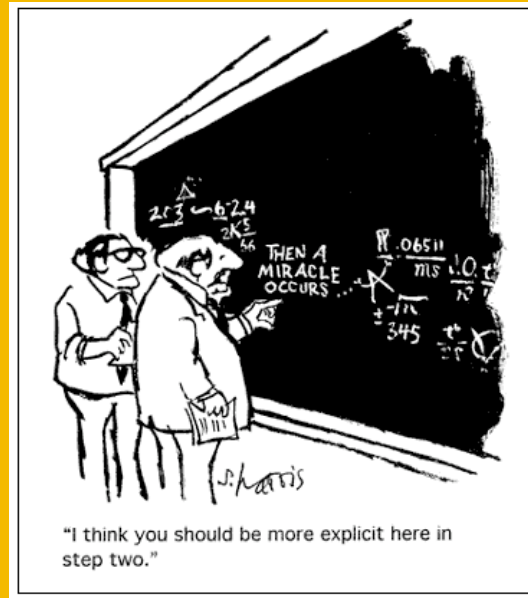
- The in-medium QCD evolution approach works over a wide variety of energies. This is, of course, expected because we have an analytic proof of the relation between QCD evolution and energy loss



Z. Kang et al. (2014)

- 4 calculations compared
- Eliminates the uncertainty associated with the application of the e-loss.
- Uncertainty from jet quenching method - constrains $\Delta g/g=5\%$
- Validates more than a decade of hadron suppression phenomenology

II. Phenomenology of light hadrons at LHC



Comment on cold nuclear matter effects

- Multiple nuclear effects play a role in the modification of the transverse momentum distributions even in p+A

- CNM energy loss

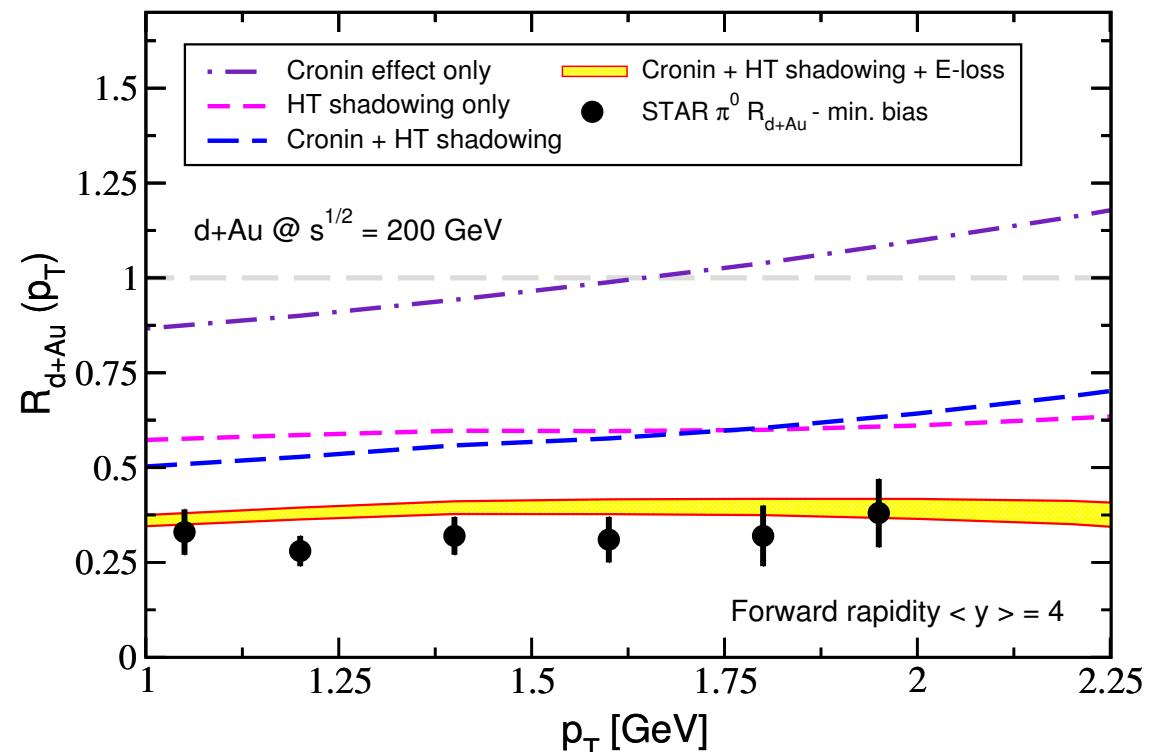
$$x_1 \rightarrow x_1 / (1 - \epsilon_{\text{eff}})$$

- Coherent power corrections

$$m_{dyn}^2 = \mu^2 A^{1/3}$$

- Cronin effect

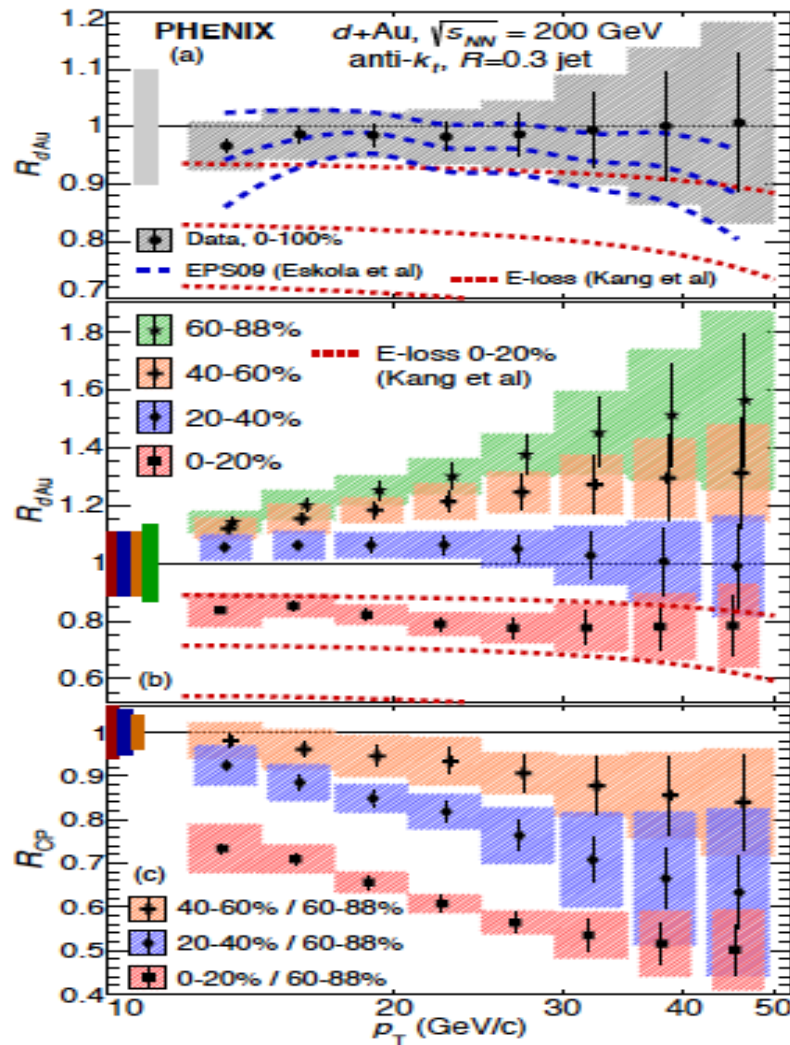
$$\langle k_T^2 \rangle_{pA} = \langle k_T^2 \rangle_{pp} + 2 \frac{\mu^2 L}{\lambda} \xi$$



B. Neufeld et al., (2010)

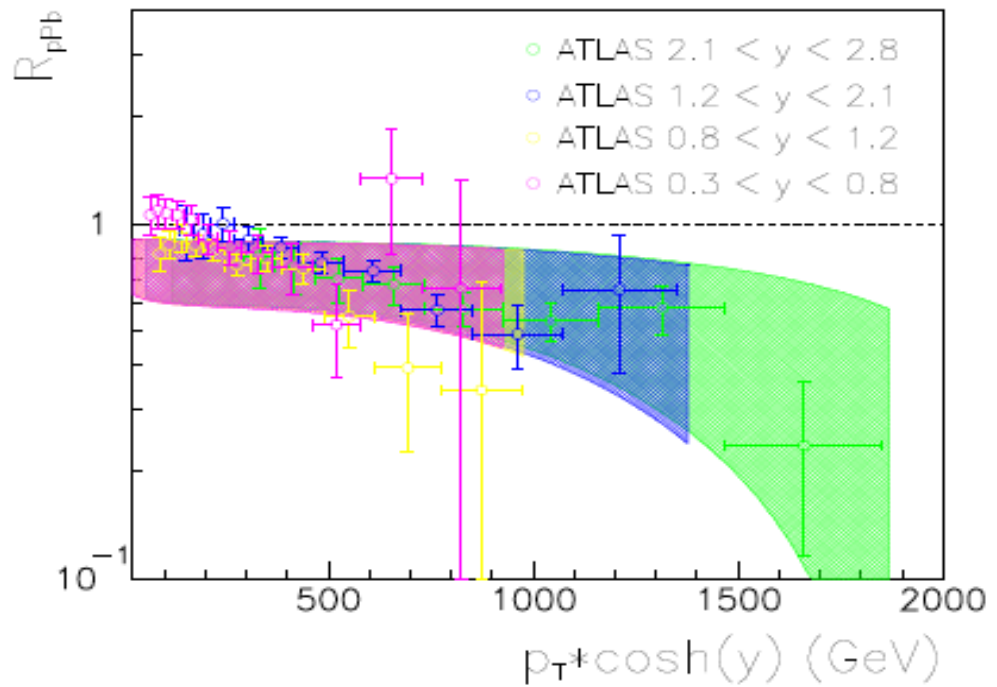
While there are uncertainties in their magnitude, it is important to include a range of CNM effects in the theoretical calculations

Example of jet production in p+A collisions at RHIC and LHC



A. Adare et al. (2015)

G. Aad et al. (2014)



Z. Kang et al . PRC (2015)

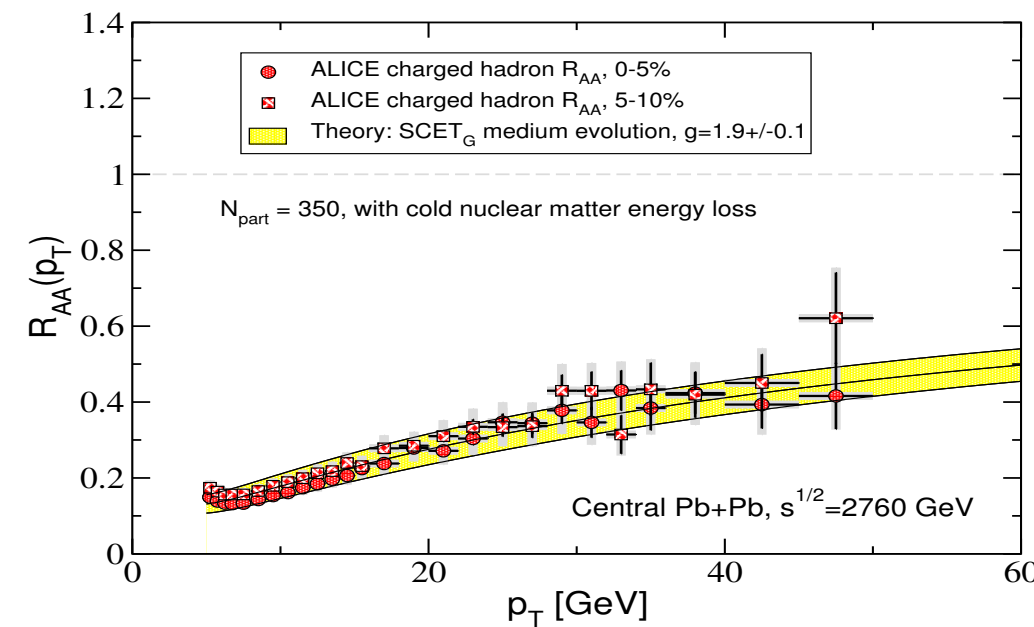
$$p_T \times \cosh(y) \propto x_a \sqrt{s}$$

- Different explanations/fits to data
- With CNM energy loss we understand the scaling, the central collisions, and are not incompatible with min bias (small effect)

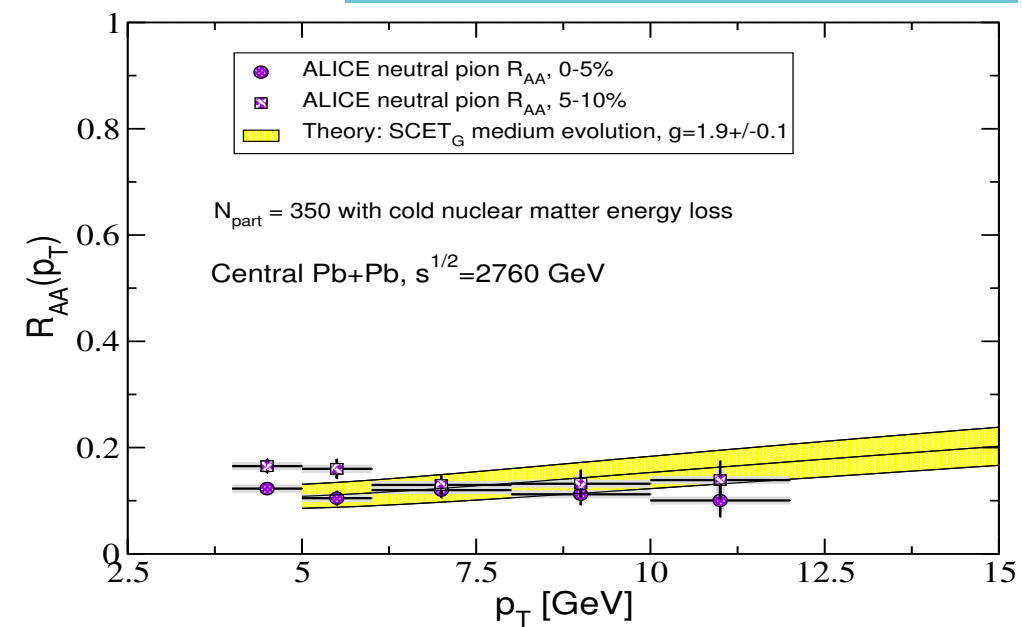
Results at the LHC 2.76 TeV

- Good description of the p_T dependence of inclusive charged particle quenching to 50 GeV. The theoretical approach is based on medium evolution with $SCET_G$ kernels.

Y.T. Chien et al. (2015)



B. Abelev et al. (2012)

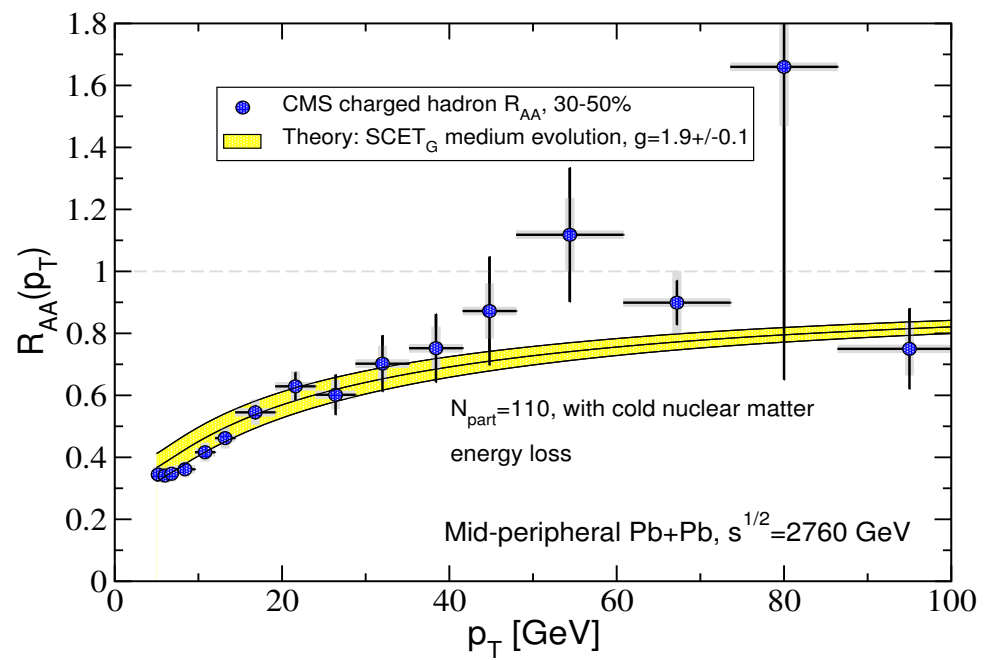
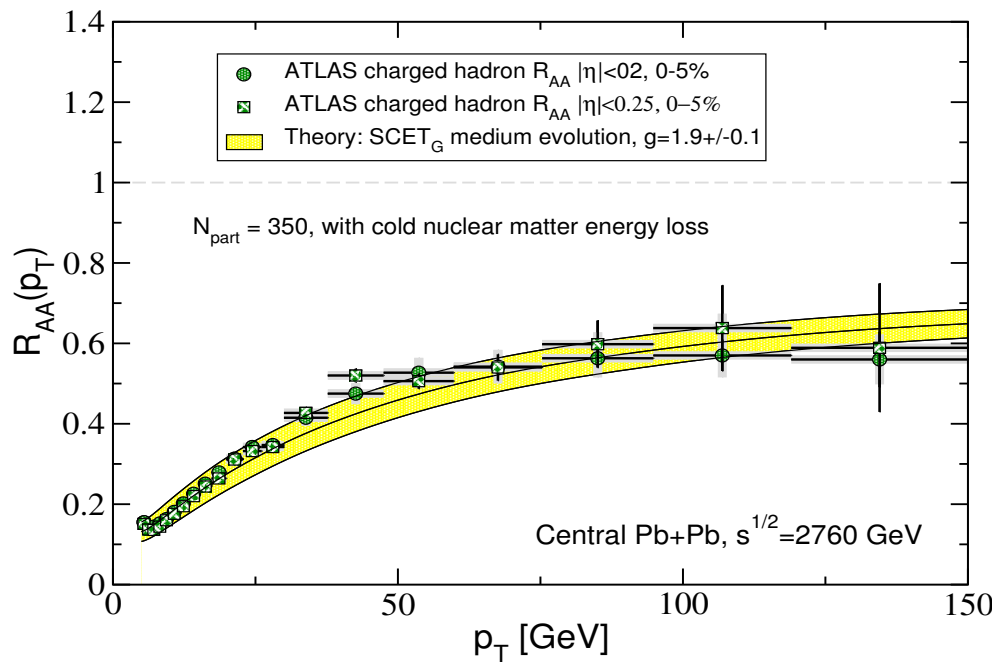


B. Abelev et al. (2014)

- We observe some discrepancy in the p_T trend of neutral pion suppression (magnitude appears well described). Important to check to higher p_T at higher CM energies at LHC run II.

Results at higher p_T and for different centralities

- The theoretical model appears to capture well the p_T and centrality dependence of inclusive hadron suppression

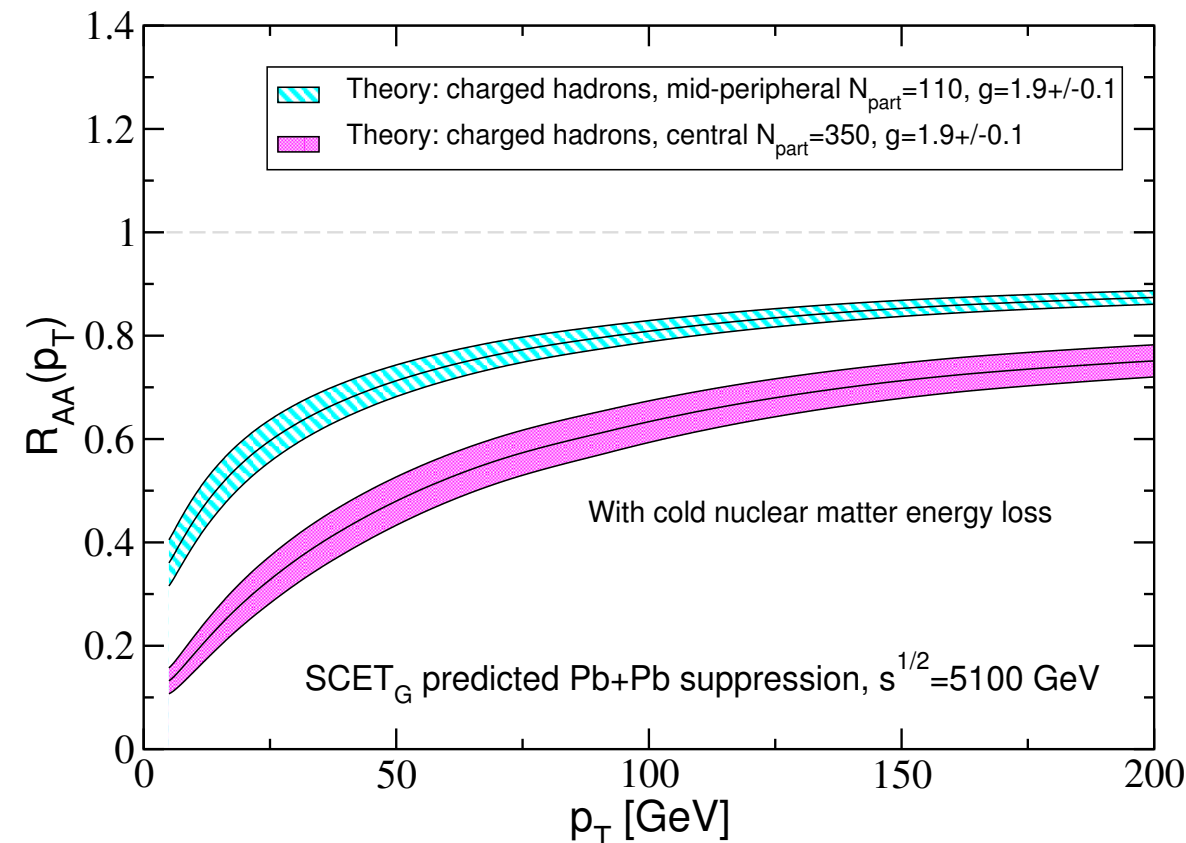


G. Aad et al. (2015)

S. Chatrchyan et al. (2012)

- At high p_T , calculations that include small nuclear matter energy loss

Predictions for the LHC 5.1 TeV run



Y.T. Chien et al. (2015)

- QCD effects run logarithmically with energy
- We account for < 10% increase in the medium density, CNM effect, fraction of quark vs gluon jets
- We find results very similar to the 2.76 TeV run, within 10% of the known R_{AA}
- At the highest transverse momenta there is sensitivity to CNM especially CNM energy loss

Prediction available for charges hadrons or neutral pions in the manuscript.
(Or send us an email)

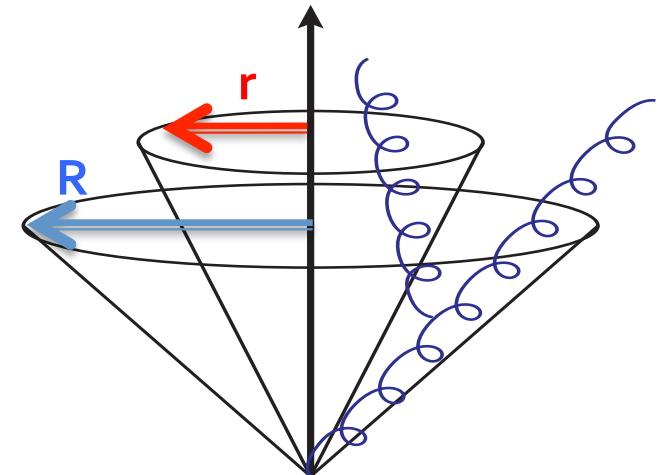
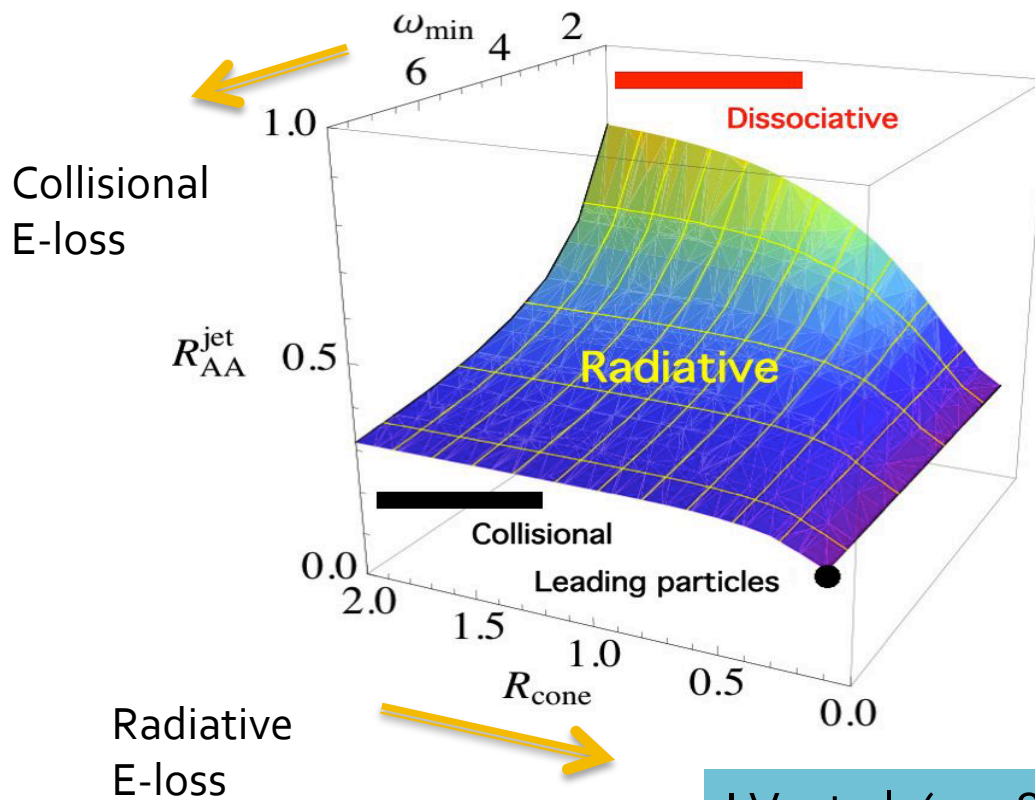
III. Jet production in HIC and jet substructure



Applications of $SCET_G$ to jet shapes and jet cross sections

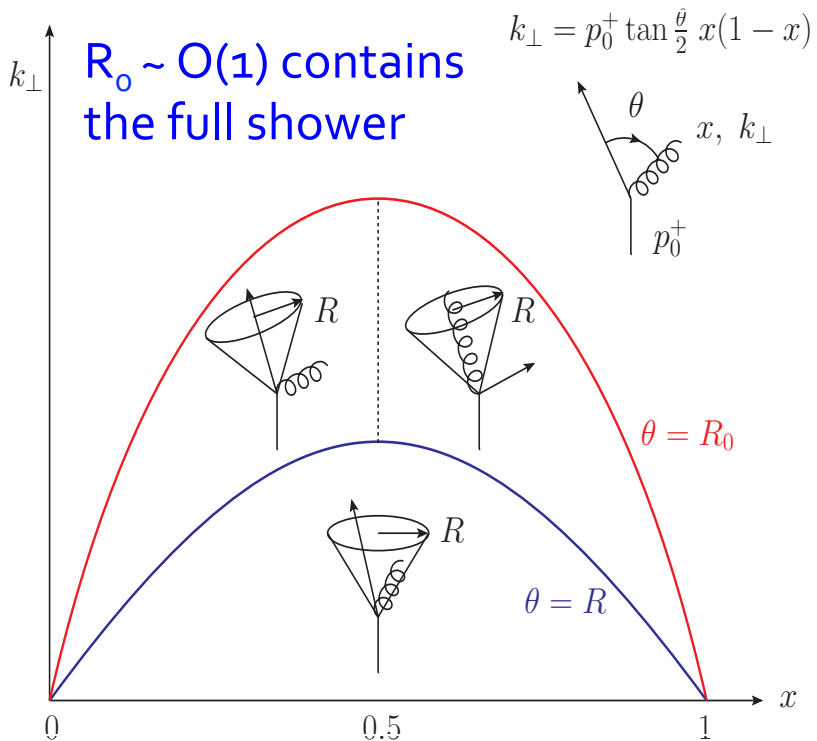
- Jet cross sections reflect the total amount of energy retained in the jet cone

- Jet shapes reflect the energy density inside the jet and the structure of the parton shower



$$\Psi_{\text{int}}(r; R) = \frac{\sum_i (E_T)_i \Theta(r - (R_{\text{jet}})_i)}{\sum_i (E_T)_i \Theta(R - (R_{\text{jet}})_i)},$$
$$\psi(r; R) = \frac{d\Psi_{\text{int}}(r; R)}{dr}.$$

Generalizing the concept of energy loss to jets



- In contrast to hadron production, the jet definition allows to generalize the concept of energy loss beyond the soft gluon approximation

Y.-T. Chien et al. (2015)

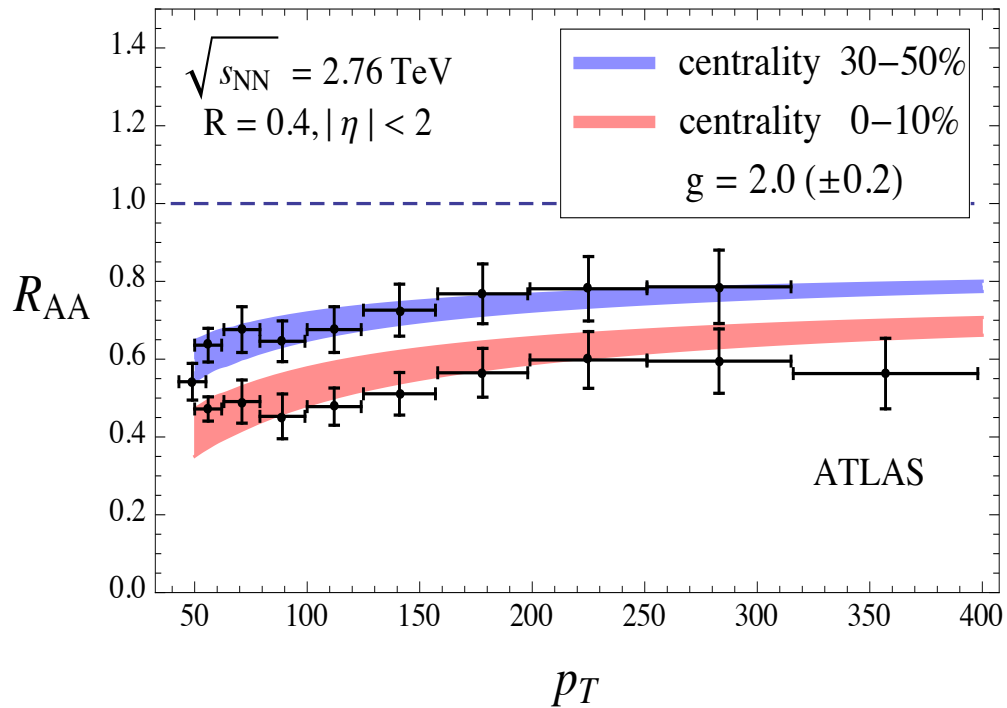
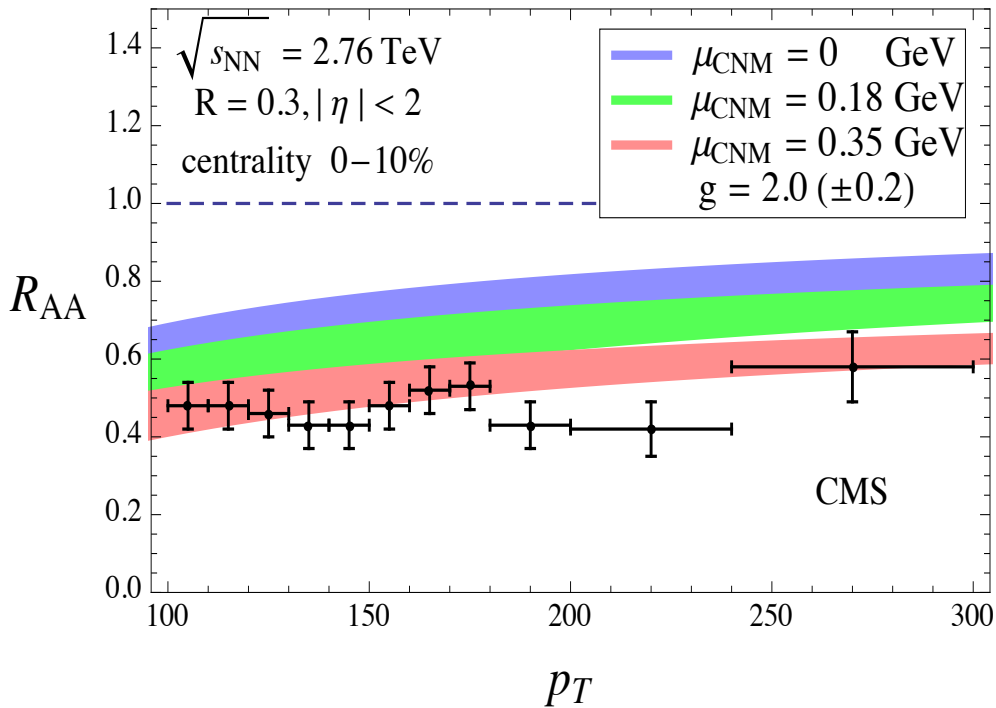
- The universal quantities – in-medium parton splitting functions come into play

$$\epsilon_q = \frac{2}{\omega} \left[\int_0^{\frac{1}{2}} dx k^0 + \int_{\frac{1}{2}}^1 dx (p^0 - k^0) \right] \int_{\omega x(1-x) \tan \frac{R_0}{2}}^{\omega x(1-x) \tan \frac{R_0}{2}} dk_{\perp} \frac{1}{2} [\mathcal{P}_{q \rightarrow qg}^{med}(x, k_{\perp}) + \mathcal{P}_{q \rightarrow gq}^{med}(x, k_{\perp})]$$

$$\epsilon_g = \frac{2}{\omega} \left[\int_0^{\frac{1}{2}} dx k^0 + \int_{\frac{1}{2}}^1 dx (p^0 - k^0) \right] \int_{\omega x(1-x) \tan \frac{R}{2} x(1-x)}^{\omega x(1-x) \tan \frac{R}{2}} dk_{\perp} \frac{1}{2} [\mathcal{P}_{g \rightarrow gg}^{med}(x, k_{\perp}) + \sum_{q,\bar{q}} \mathcal{P}_{g \rightarrow q\bar{q}}^{med}(x, k_{\perp})]$$

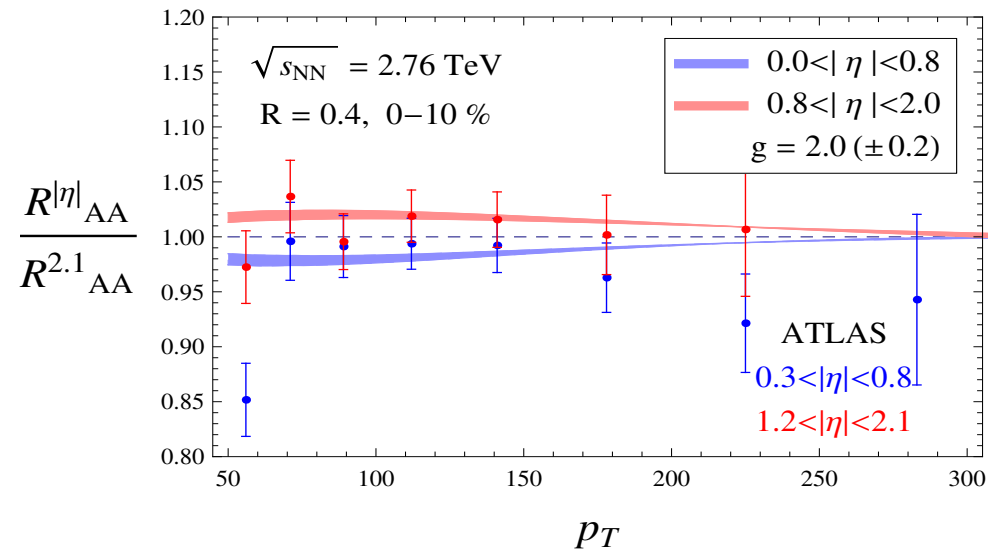
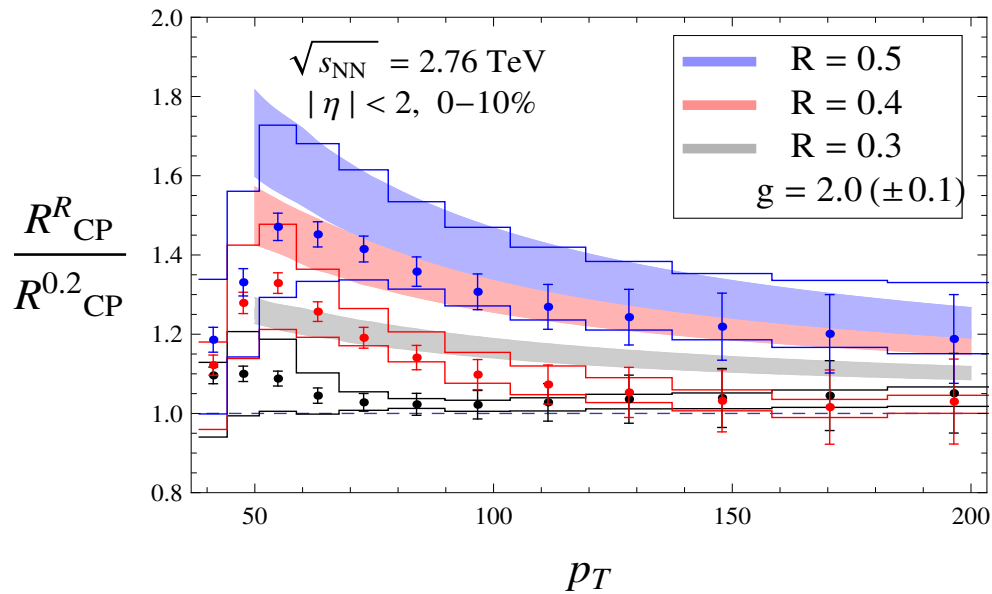
Fractional energy loss outside of the jet beyond the soft gluon approximation

Suppression of reconstructed jets at the LHC, Pb+Pb at 2.76 TeV



- Cold nuclear matter effects contribute toward the inclusive jet suppression at very high p_T . Approximately $\frac{1}{2}$ of the effect
- Describes well the centrality dependence of the inclusive jet suppression
- There is some p_T dependence remaining to R_{AA} . Important to investigate soft function effects, collisional energy loss

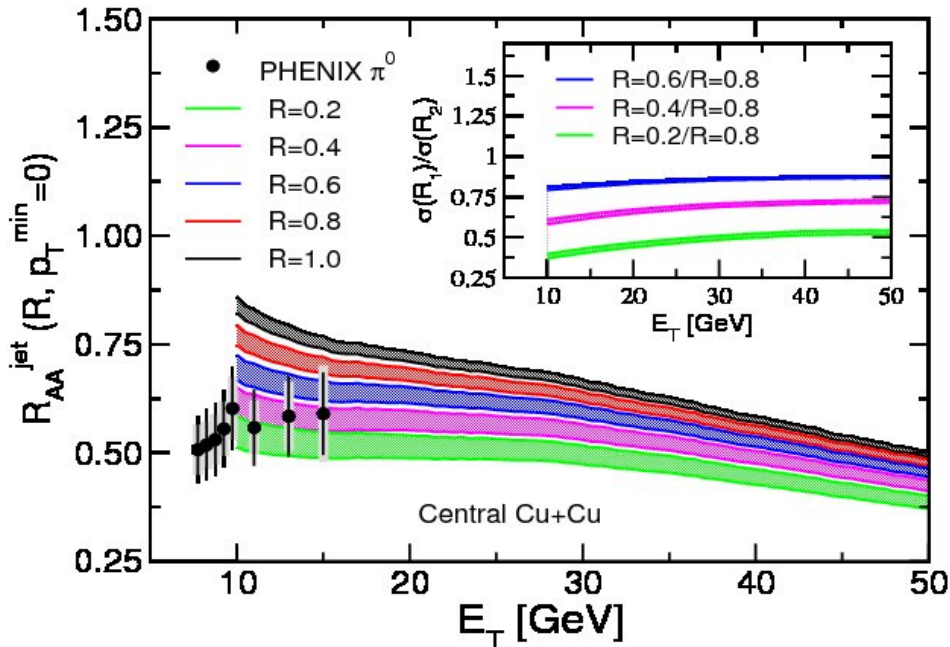
Jet radius and rapidity dependence of inclusive jet suppression



$$R_{cp}^R(p_T) = \langle N_{\text{bin}}^{\text{per}} \rangle \frac{d\sigma_{AA}^{\text{cen}}(p_T, R)}{dyd^2p_T} / \langle N_{\text{bin}}^{\text{cen}} \rangle \frac{d\sigma_{AA}^{\text{per}}(p_T, R)}{dyd^2p_T} = \frac{R_{AA}^{\text{cen}}(p_T, R)}{R_{AA}^{\text{per}}(p_T, R)}$$

- The radius dependence of inclusive jet quenching versus p_T and R captured. For small radii the calculation over predicts the differences
- Rapidity dependence is consistent with 1. The trend is captured by the theoretical calculation

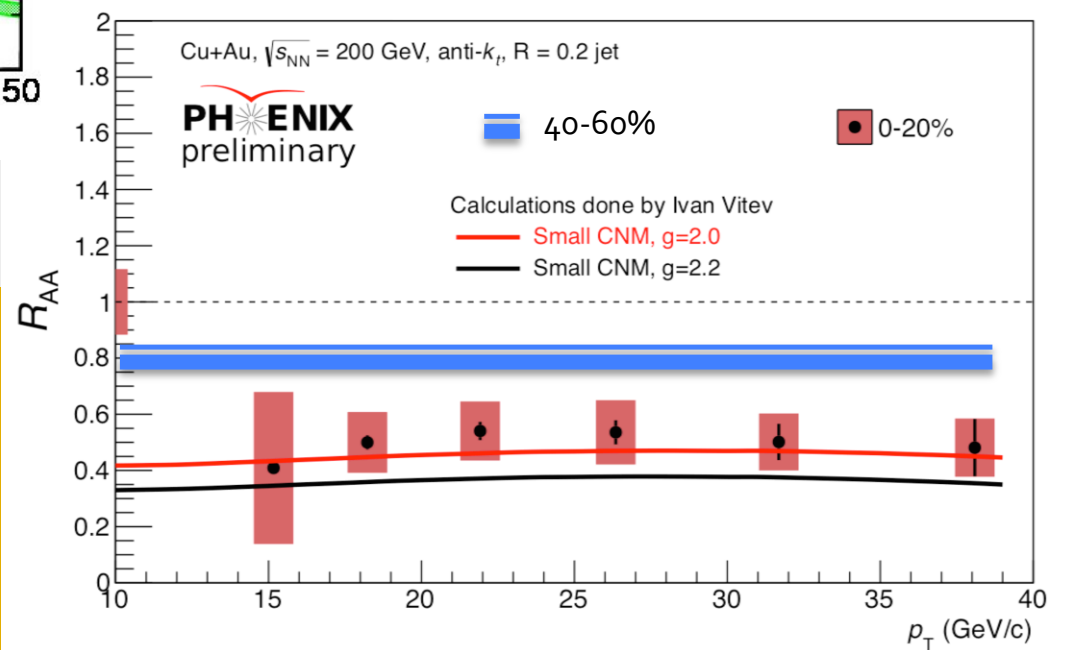
Suppression of reconstructed jets at RHIC



I.V. et al. (2009)

- We have updated the calculation using SCET_G parton showers beyond the soft gluon emission limit
- RHIC preliminary results are available. See talk by Arbin

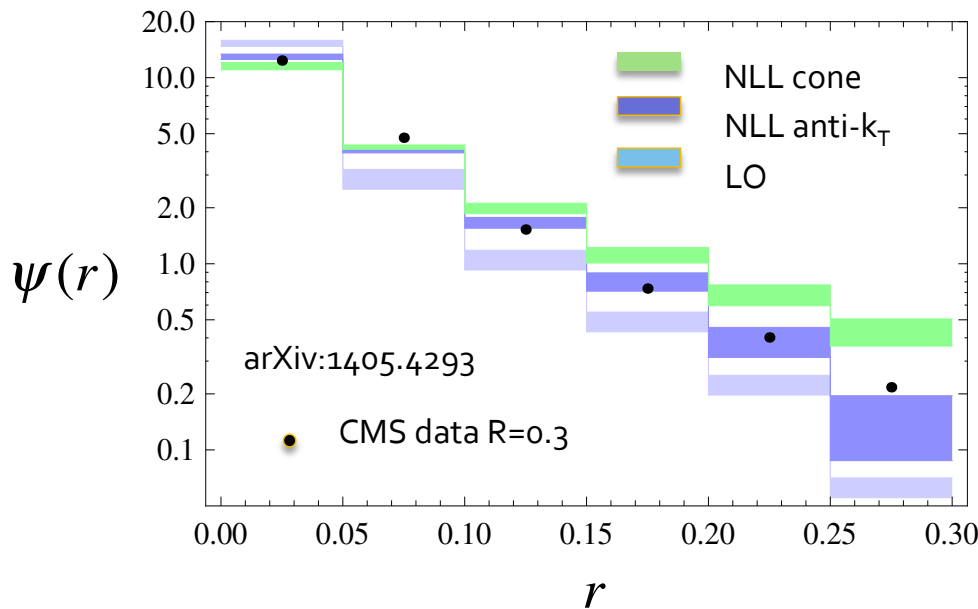
- RHIC offer increased sensitivity to QGP transport properties and CNM effects
- Much steeper falling spectra, more than offset the effects of smaller density and more quark jets
- Original predictions done in the energy loss approach



A. Timilsina, private communication (2015)

NLL calculation of jet shapes

- The jet shape is defined by the ratio of two jet energy functions



$$\Psi_\omega(r) = \frac{\langle E_r \rangle_\omega}{\langle E_R \rangle_\omega} = \frac{J_\omega^{E_r}(\mu)/J_\omega(\mu)}{J_\omega^{E_R}(\mu)/J_\omega(\mu)} = \frac{J_\omega^{E_r}(\mu)}{J_\omega^{E_R}(\mu)}$$

- To resum the jet shape to NLL accuracy we use SCET RG evolution techniques

$$\frac{dJ_\omega^{qE_r}(\mu)}{d\ln\mu} = \left[-C_F \Gamma_{\text{cusp}}(\alpha_s) \ln \frac{\omega^2 \tan^2 \frac{R}{2}}{\mu^2} - 2\gamma^q(\alpha_s) \right] J_\omega^{qE_r}(\mu)$$

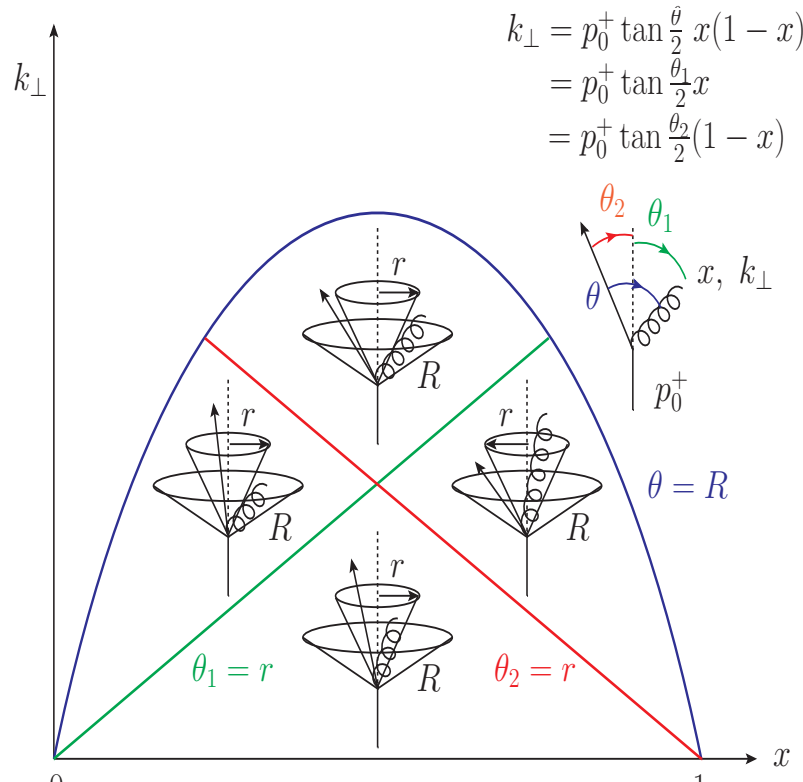
$$\frac{dJ_\omega^{gE_r}(\mu)}{d\ln\mu} = \left[-C_A \Gamma_{\text{cusp}}(\alpha_s) \ln \frac{\omega^2 \tan^2 \frac{R}{2}}{\mu^2} - 2\gamma^g(\alpha_s) \right] J_\omega^{gE_r}(\mu)$$

- We derived the algorithm dependence of the jet shapes (anti) k_T vs cone
- Significant improvement over fixed order calculation

| NLL | 1-loop | 2-loop |
|------------------------|--|--|
| β | $\beta_0 = \frac{11}{3}C_A - \frac{4}{3}T_F n_f$ | $\beta_1 = \frac{34}{3}C_A^2 - \frac{20}{3}C_A T_F n_f - 4C_F T_F n_f$ |
| Γ_{cusp} | $\Gamma_0 = 4$ | $\Gamma_1 = 4 \left[\left(\frac{67}{9} - \frac{\pi^2}{3} \right) C_A - \frac{20}{9} T_F n_f \right]$ |
| γ | $\gamma_0^q = -3C_F, \gamma_0^g = -\beta_0$ | |

Y.-T. Chien et al. (2014)

Medium-modified jet shapes at NLL



$$E_r(x, k_\perp) = \mathcal{M}_1 + \mathcal{M}_2 + \mathcal{M}_3 + \mathcal{M}_4$$

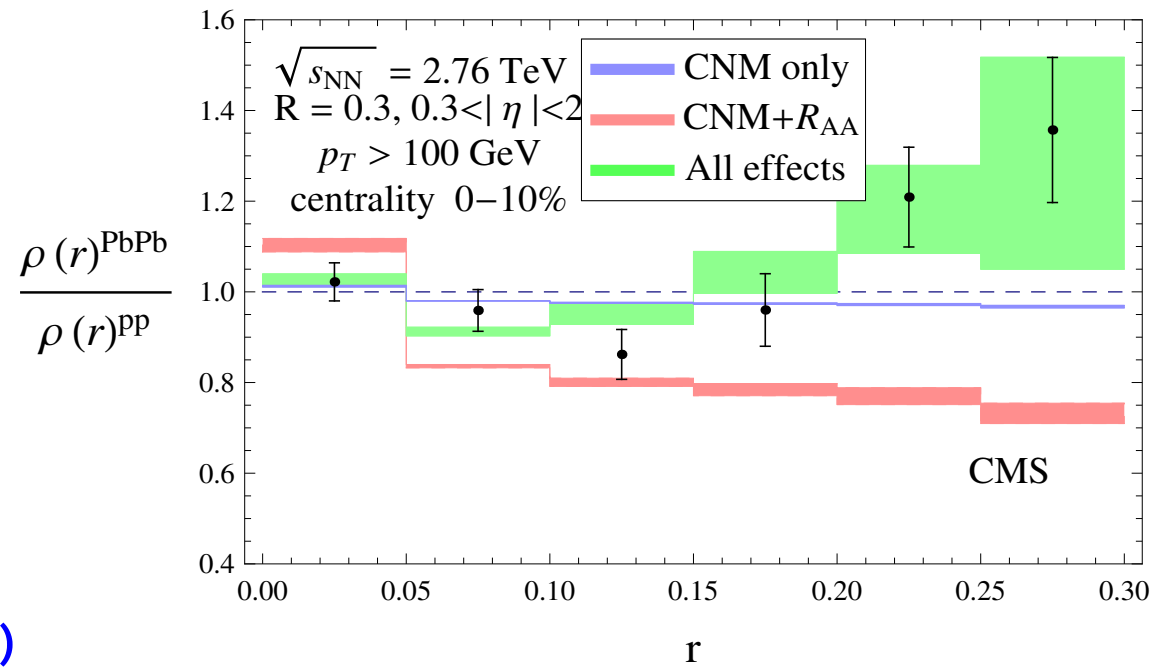
Measurement operator – tells us how the above configurations contribute energy to J (jet function)

$$\begin{aligned} k_\perp &= p_0^+ \tan \frac{\theta}{2} x(1-x) \\ &= p_0^+ \tan \frac{\theta_1}{2} x \\ &= p_0^+ \tan \frac{\theta_2}{2} (1-x) \end{aligned}$$

- One can evaluate the jet energy functions from the splitting functions

$$J_{\omega, E_r}^i(\mu) = \sum_{j,k} \int_{PS} dx dk_\perp \mathcal{P}_{i \rightarrow jk}(x, k_\perp) E_r(x, k_\perp)$$

$$J_{\omega, E_r}(\mu) = J_{\omega, E_r}^{vac}(\mu) + J_{\omega, E_r}^{med}(\mu).$$



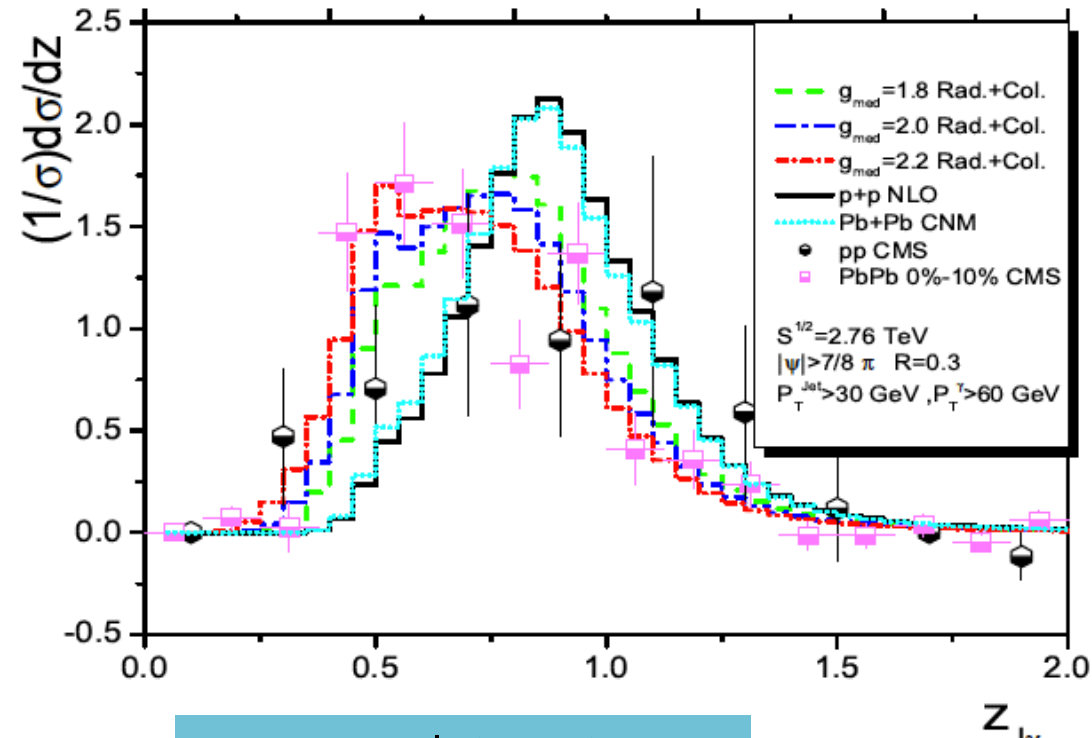
- First quantitative pQCD/SCET description of jet shapes in HI

γ -tagged jet momentum imbalance

- Photon tagging (isolated photons) does not induce bias
- The momentum imbalance shift can be related on average to fractional energy loss
- The inverse Compton scattering process selects quark jets (smaller quenching, imbalance)

$$\langle z_{j\gamma} \rangle = \left(\int dz_{j\gamma} z_{j\gamma} \frac{d\sigma}{dz_{j\gamma}} \right) / \left(\int dz_{j\gamma} \frac{d\sigma}{dz_{j\gamma}} \right)$$

| | γ -light jet |
|-------------|---------------------|
| p+p | .94 |
| Pb+Pb g=2 | .84 (-11%) |
| Pb+Pb g=2.2 | .71 (-24%) |



W. Dai et al. (2012)

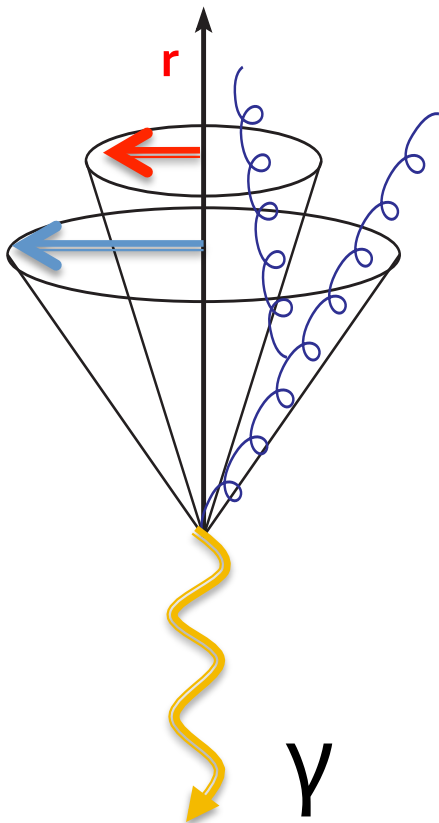
Momentum imbalance of photon-tagged jets

$$Z_J = \frac{p_{T_{jet}}}{p_{T_\gamma}}$$

$$\frac{d\sigma}{dz_{J\gamma}} = \int_{p_{T_{jet}}^{min}}^{p_{T_{jet}}^{max}} dp_{T_{jet}} \frac{p_{T_{jet}}}{z_{J\gamma}^2} \frac{d\sigma[z_{J\gamma}, p_{T_\gamma}(z_{J\gamma}, p_{T_{jet}})]}{dp_{T_\gamma} dp_{T_{jet}}}$$

Predictions for the 5.1 TeV Pb+Pb run at the LHC

- We extend predictions (beyond the soft gluon approximation) for other observables – photon tagged jets and photon tagged jet shapes

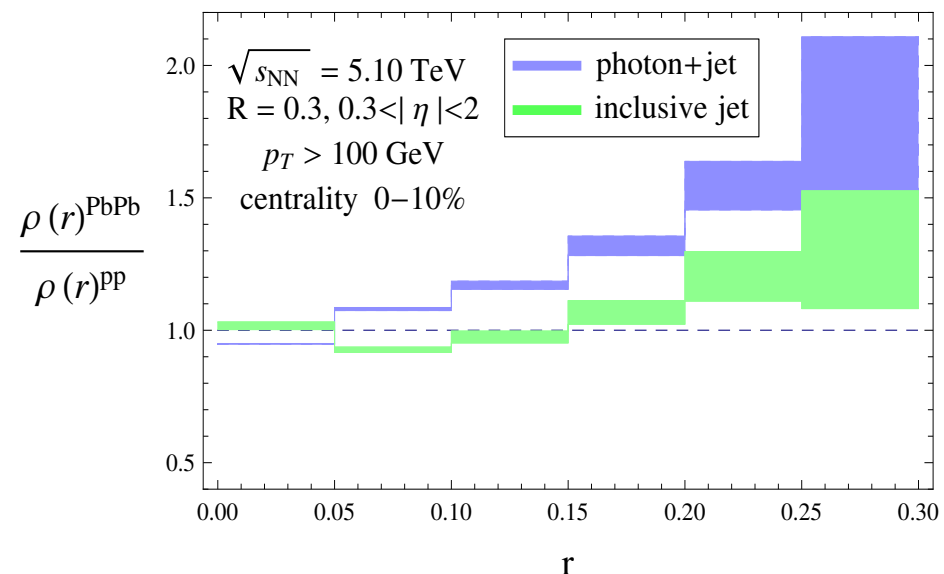
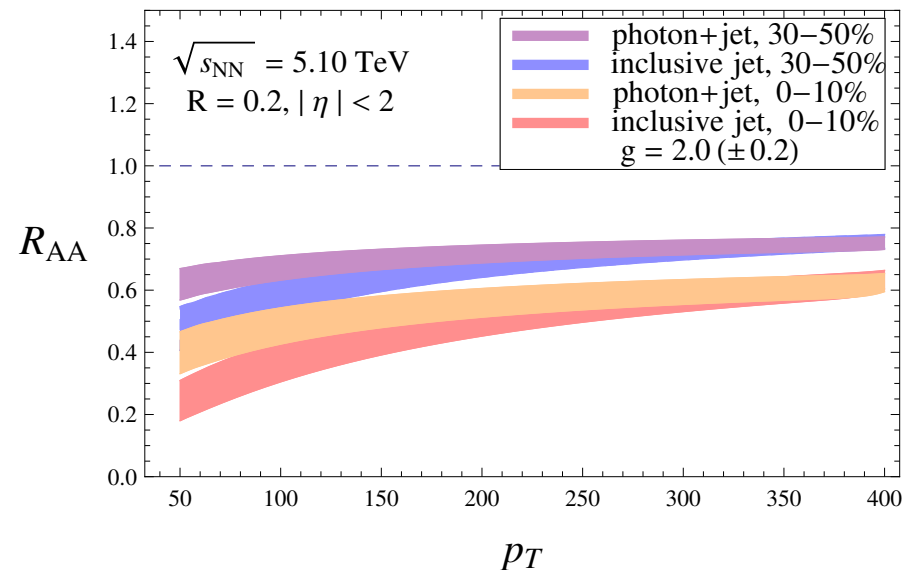


Photon tagging allows to alter/control the recoil jet composition

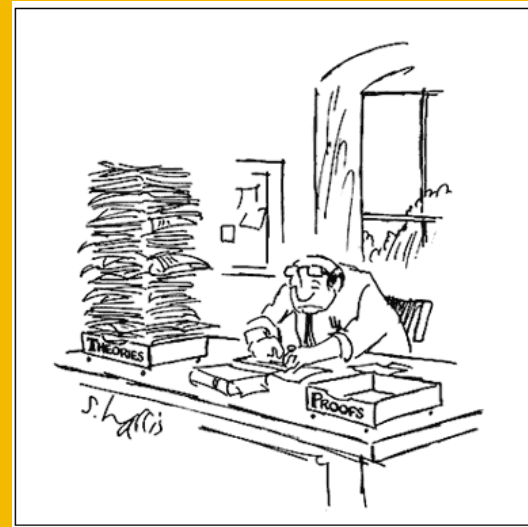
Measurable differences are predicted in the jet suppression at low p_T

Significant differences are expected in the jet shapes

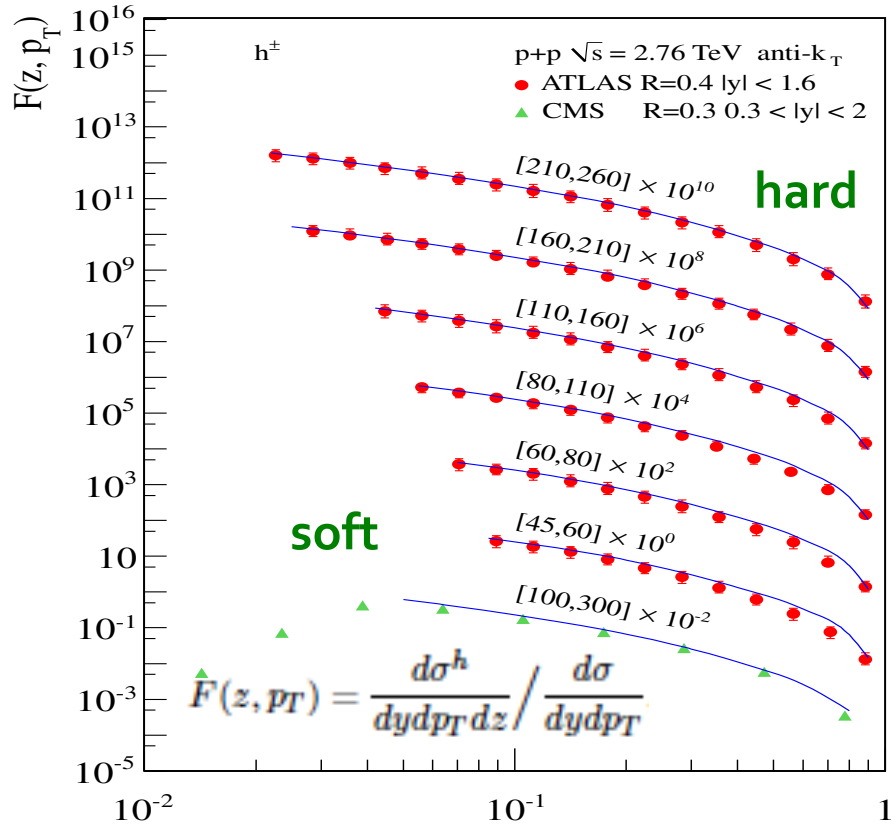
Y.-T. Chien et al. (2015)



IV. New topics in perturbative jet theory



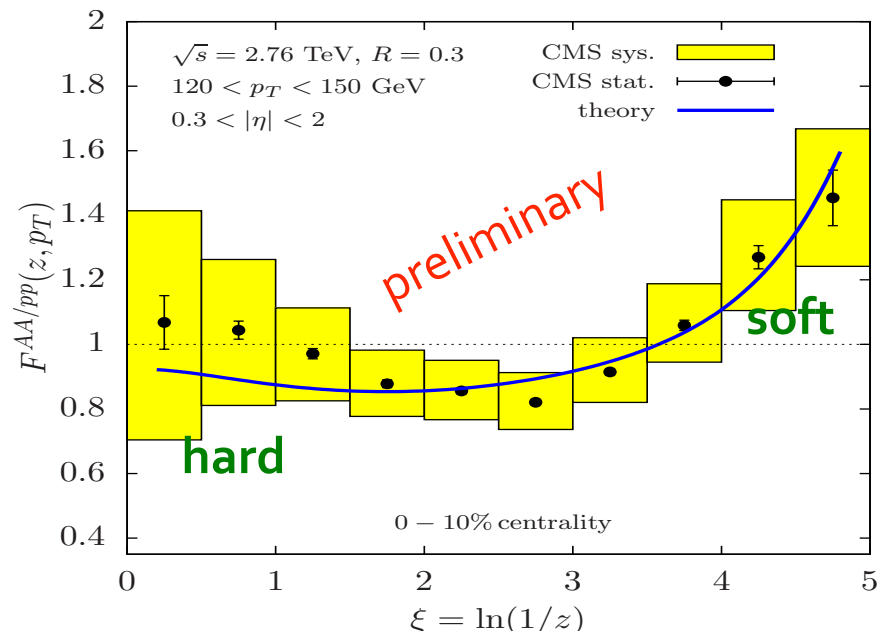
Jet fragmentation functions at LHC



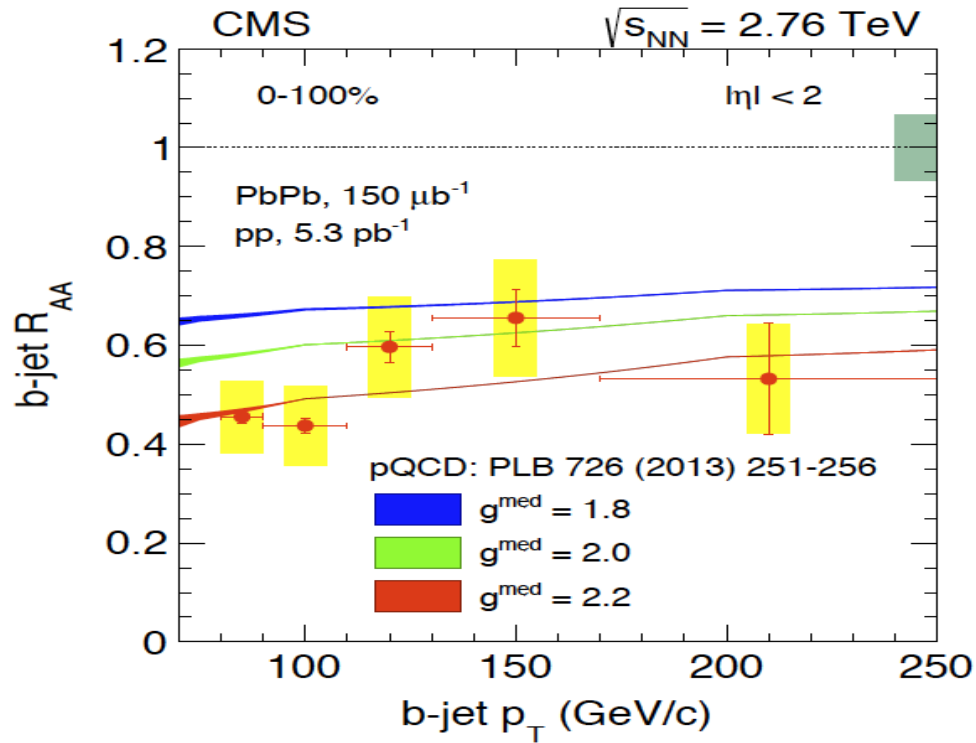
We talk by F. Ringer about extended discussion of jet fragmentation functions on $p+p$ from SCET, uncertainties and preliminary results for A+A

Y-T. Chien et al. (2015)

- A factorized expression can be written in SCET, analogously to jet shapes
- Very good comparison to data for z not too small and light hadrons. Both MC and pQCD /SCET fail for heavy flavor
- Preliminary results in A+A reactions qualitatively consistent with data. Large uncertainties associated with the FFs



B-jet suppression

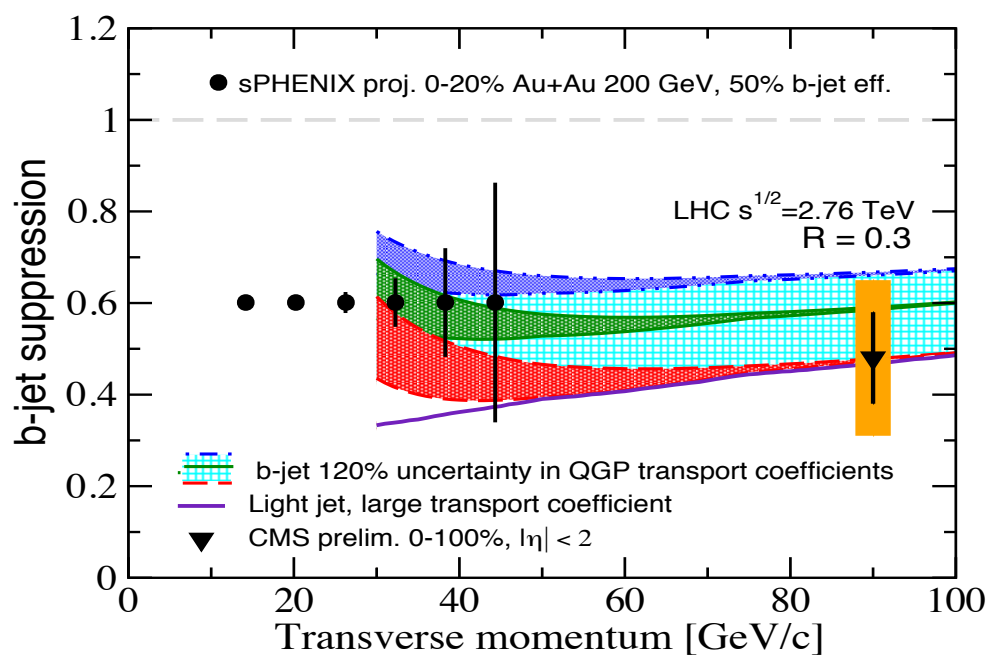


S. Chatrchyan et al et al. (2014)

J. Huang et al et al. (2013)

Wee talk by H. Xing about extended discussion of b-jet theory, tagged b-jets and channels that can increase the b-jet purity

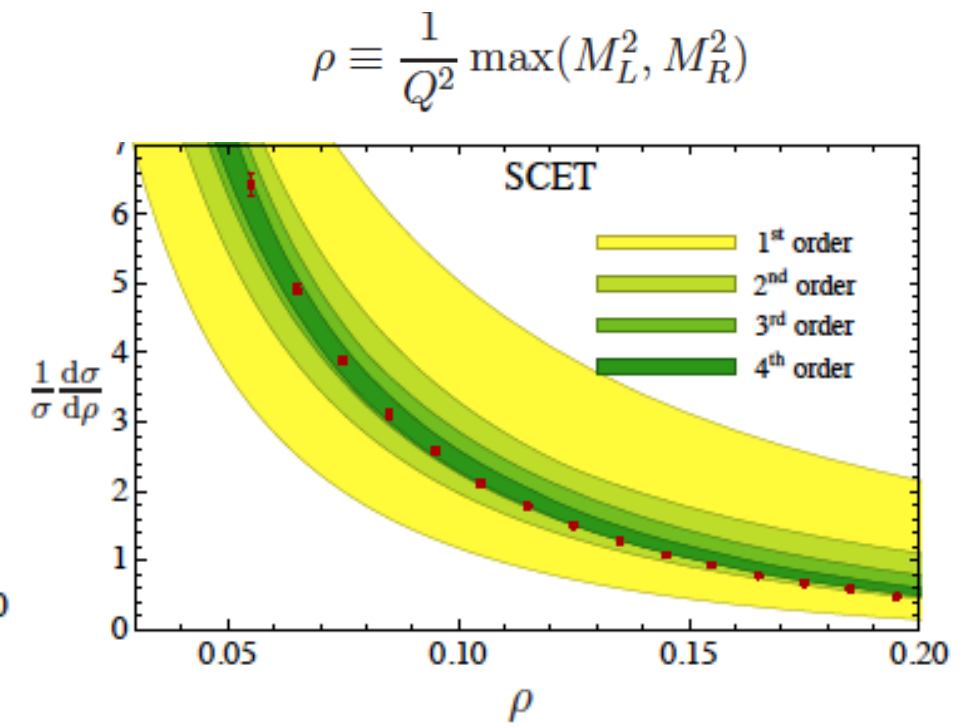
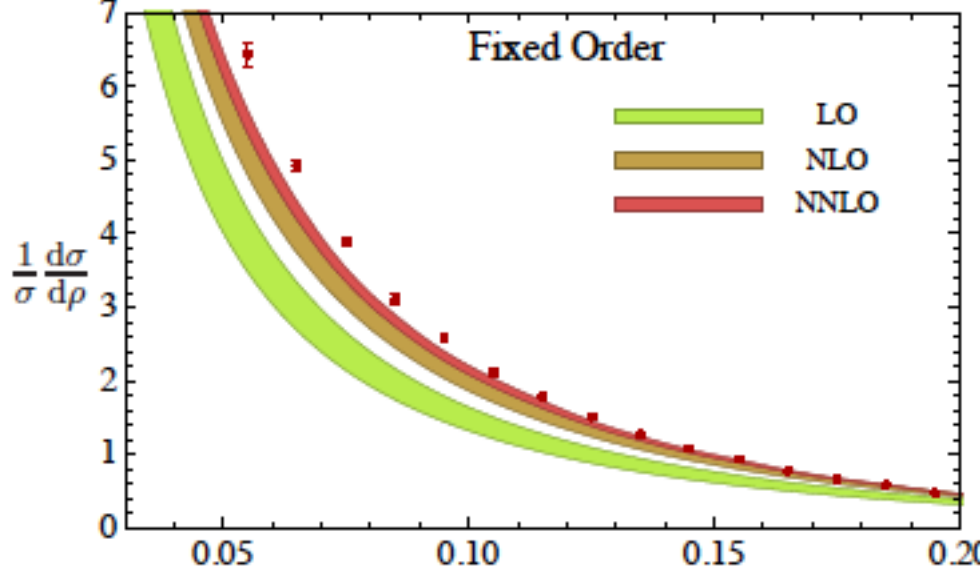
- Include cold nuclear matter effects
- At high p_T the suppression of b-jets is very very similar to that of light jets (but subtle to evaluate)
- At $p_T < 50 \text{ GeV}$ the difference is due to the mass effect
- This is the region to look at with LHC run II and sPHENIX



Jet mass distributions

- Jet mass distribution, example of accuracy of SCET resummation NNNLL accuracy

$$\frac{1}{\sigma_0} \frac{d^2\sigma_2}{dM_L^2 dM_R^2} = H(Q^2, \mu) \int dk_L dk_R J(M_L^2 - Qk_L, \mu) J(M_R^2 - Qk_R, \mu) S(k_L, k_R, \mu)$$



Wee talk by Y.T Chien about precision theory of jet mass distributions

Y.T Chien et al. (2010)

Conclusions

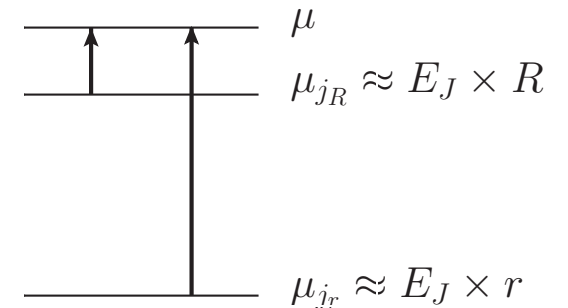
- An effective theory of jet propagation in matter $SCET_G$ was constructed (collinear sector). All medium-induced parton splittings derived, factorization and gauge invariance proven
- The connection between the traditional energy loss phenomenology and the QCD evolution/parton shower approach to jet quenching now established. Very good description of inclusive hadron suppression obtained, predictions for the 5.1 TeV run given
- The differences in jet quenching between 2.76 TeV and 5.1 TeV is small. What the LHC Pb+Pb run II allows is better statistics, higher p_T and new channels
- First SCET calculation of jet shapes performed to NLL accuracy. Improved predictions for p+p collisions. More work needed to understand heavy flavor
- Calculations of jet cross sections and jet shapes are now available beyond the energy loss approach. Comparable description of inclusive jet suppression to the energy loss approach. Much improved description of jet shape modification.
- Photon-tagged jets allow us to get insights into the flavor dependence of jet quenching.
- Important topics to be covered at this workshop: fragmenting jet functions, heavy flavor and heavy flavor jets, precision theory and jet mass distributions

NLL calculation of jet shapes

- We use SCET resummation techniques and SCET_G.

We start from the natural scales that eliminate all large logarithms in the fixed order calculation and evolve to a common scale [resumming $\ln(r/R)$]

- To resum the jet shape to NLL accuracy



$$\frac{dJ_\omega^{qE_r}(\mu)}{d\ln\mu} = \left[-C_F \Gamma_{\text{cusp}}(\alpha_s) \ln \frac{\omega^2 \tan^2 \frac{R}{2}}{\mu^2} - 2\gamma^q(\alpha_s) \right] J_\omega^{qE_r}(\mu)$$

$$\frac{dJ_\omega^{gE_r}(\mu)}{d\ln\mu} = \left[-C_A \Gamma_{\text{cusp}}(\alpha_s) \ln \frac{\omega^2 \tan^2 \frac{R}{2}}{\mu^2} - 2\gamma^g(\alpha_s) \right] J_\omega^{gE_r}(\mu)$$

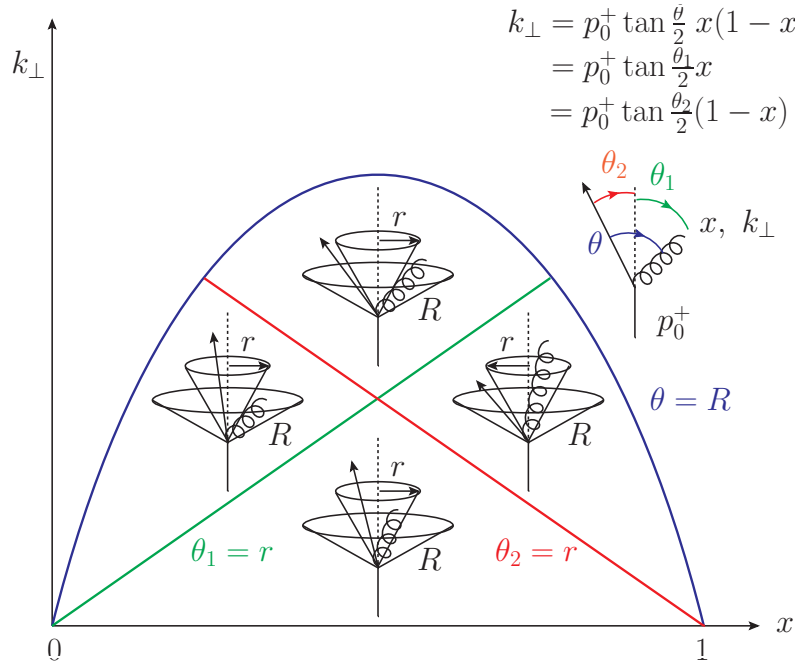
$$\Gamma_{\text{cusp}}(\alpha_s) = \left(\frac{\alpha_s}{4\pi}\right)\Gamma_0 + \left(\frac{\alpha_s}{4\pi}\right)^2\Gamma_1 + \dots,$$

$$\gamma(\alpha_s) = \left(\frac{\alpha_s}{4\pi}\right)\gamma_0 + \left(\frac{\alpha_s}{4\pi}\right)^2\gamma_1 + \dots.$$

| Order | Γ_{cusp} | γ | β |
|-------|------------------------|----------|---------|
| NLL | 2-loop | 1-loop | 2-loop |

| NLL | 1-loop | 2-loop |
|------------------------|--|--|
| β | $\beta_0 = \frac{11}{3}C_A - \frac{4}{3}T_F n_f$ | $\beta_1 = \frac{34}{3}C_A^2 - \frac{20}{3}C_A T_F n_f - 4C_F T_F n_f$ |
| Γ_{cusp} | $\Gamma_0 = 4$ | $\Gamma_1 = 4 \left[\left(\frac{67}{9} - \frac{\pi^2}{3} \right) C_A - \frac{20}{9} T_F n_f \right]$ |
| γ | $\gamma_0^q = -3C_F, \gamma_0^g = -\beta_0$ | |

Phase space for the jet energy distribution



- To first non-trivial order, the phase space for the jet shape contributions is tractable

Y.-T. Chien et al. (2014)

- Define a jet energy function

$$J_{\omega}(E_r, \mu) = \sum_{X_c} \langle 0 | \bar{\chi}_{\omega}(0) | X_c \rangle \langle X_c | \chi_{\omega}(0) | 0 \rangle \delta(E_r - \hat{E}^{< r}(X_c))$$

- Need the distribution of the average energy

$$J_{\omega}^{E_r}(\mu) = \int dE_r E_r J_{\omega}(E_r, \mu)$$

- Integral jet function

$$\Psi_{\omega}(r) = \frac{\langle E_r \rangle_{\omega}}{\langle E_R \rangle_{\omega}} = \frac{J_{\omega}^{E_r}(\mu)/J_{\omega}(\mu)}{J_{\omega}^{E_R}(\mu)/J_{\omega}(\mu)} = \frac{J_{\omega}^{E_r}(\mu)}{J_{\omega}^{E_R}(\mu)}$$

$$\frac{2}{\omega} J_{\omega}^{q E_r}(\mu) = \alpha_s \left[a \ln^2 \frac{\omega^2 \tan^2 \frac{r}{2}}{\mu^2} + b \ln \frac{\omega^2 \tan^2 \frac{r}{2}}{\mu^2} + \text{finite} \right]$$

Solution to the resummed jet shape

- Define

$$S(\nu, \mu) = - \int_{\alpha_s(\nu)}^{\alpha_s(\mu)} d\alpha \frac{\Gamma_{\text{cusp}}(\alpha)}{\beta(\alpha)} \int_{\alpha_s(\nu)}^{\alpha} \frac{d\alpha'}{\beta(\alpha')} ,$$

$$A_i(\nu, \mu) = - \int_{\alpha_s(\nu)}^{\alpha_s(\mu)} d\alpha \frac{\gamma^i(\alpha)}{\beta(\alpha)} , \quad A_{\Gamma}(\nu, \mu) = - \int_{\alpha_s(\nu)}^{\alpha_s(\mu)} d\alpha \frac{\Gamma_{\text{cusp}}(\alpha)}{\beta(\alpha)} ,$$

- Jet function

$$J_{\omega}^{iE_r}(\mu) = J_{\omega}^{iE_r}(\mu_{j_r}) \exp [-2C_i S(\mu_{j_r}, \mu) + 2A_i(\mu_{j_r}, \mu)] \left(\frac{\omega^2 \tan^2 \frac{R}{2}}{\mu_{j_r}^2} \right)^{C_i A_{\Gamma}(\mu_{j_r}, \mu)}$$

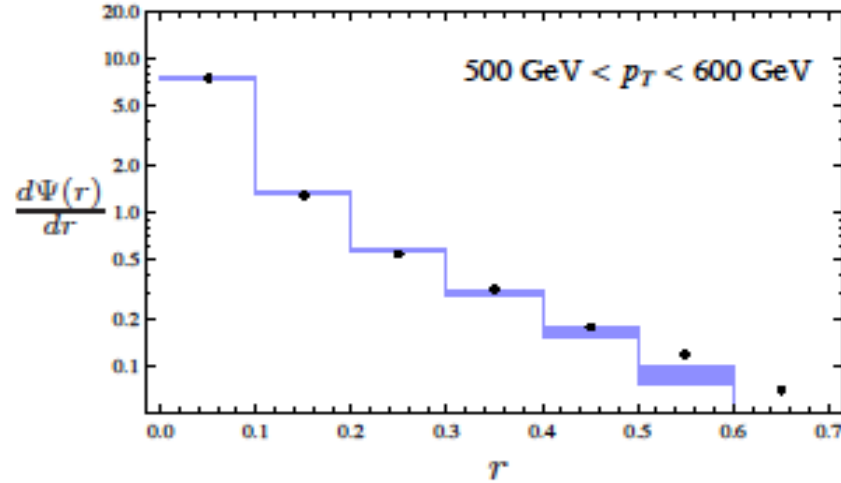
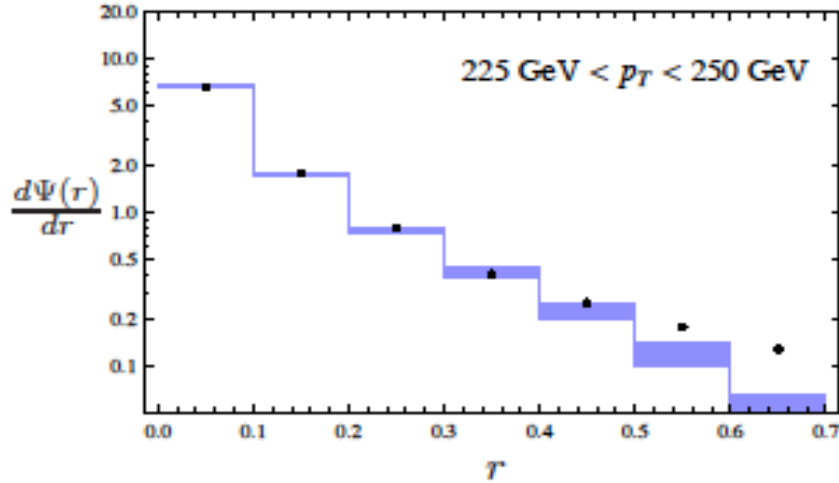
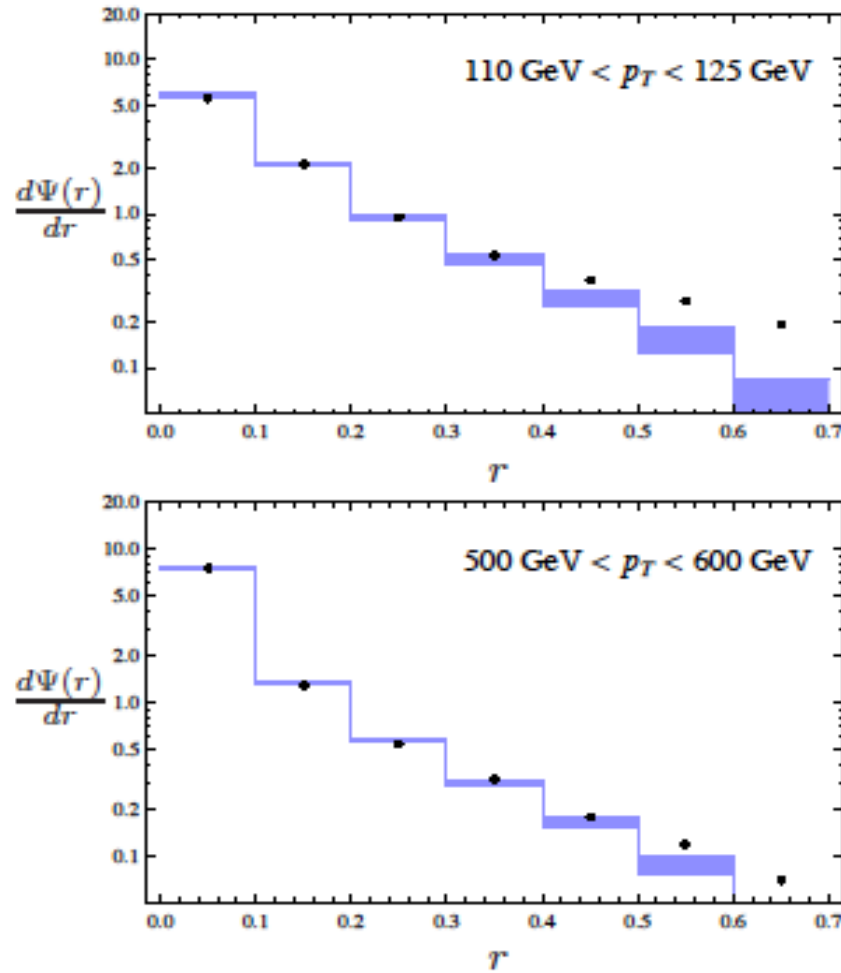
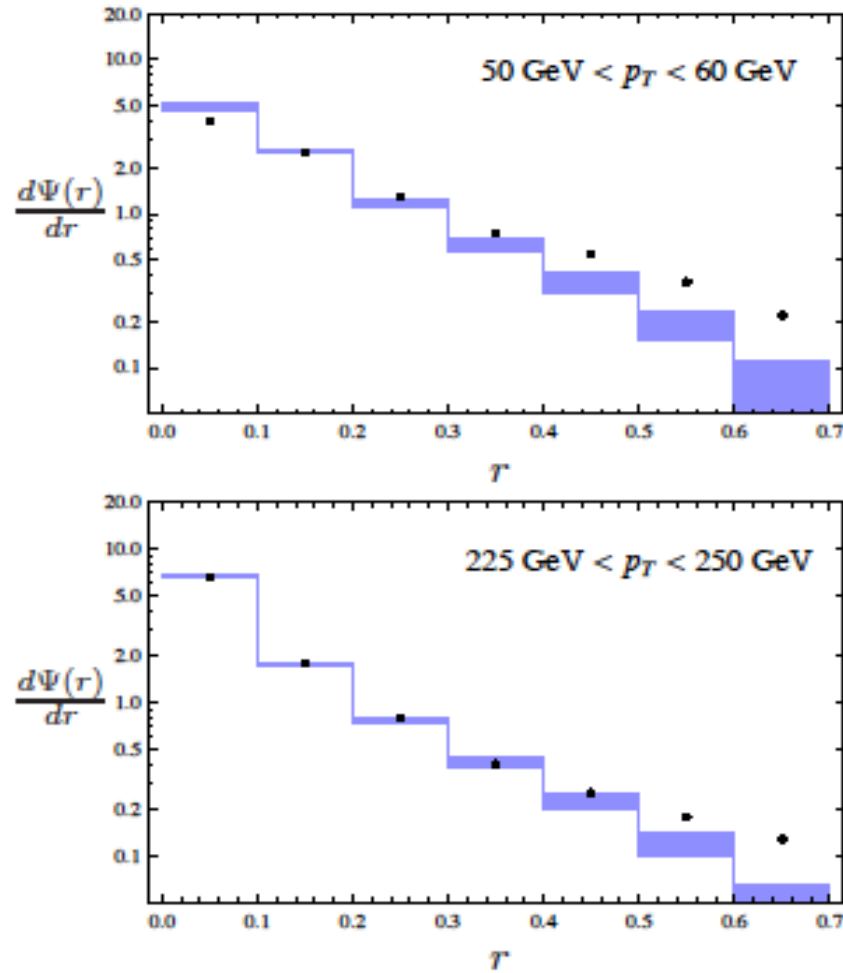
- Integral jet shape

$$\Psi_{\omega}^i(r) = \frac{J_{\omega}^{iE_r}(\mu)}{J_{\omega}^{iE_R}(\mu)} = \frac{J_{\omega}^{iE_r}(\mu_{j_r})}{J_{\omega}^{iE_R}(\mu_{j_R})} \exp [-2C_i S(\mu_{j_r}, \mu_{j_R}) + 2A_i(\mu_{j_r}, \mu_{j_R})] \times \left(\frac{\mu_{j_r}^2}{\omega^2 \tan^2 \frac{R}{2}} \right)^{C_i A_{\Gamma}(\mu_{j_R}, \mu_{j_r})}$$

Y.-T.Chien et al. (2014)

We start from the natural scales that eliminate all large logarithms in the fixed order calculation and evolve to a common scale [resumming $\ln(r/R)$]

Limitations of the calculation



- Deviations at large R and/or small energy

NLL calculation of jet shapes

- We use SCET resummation techniques and SCET_G.

$$\Psi_\omega(r) = \frac{\langle E_r \rangle_\omega}{\langle E_R \rangle_\omega} = \frac{J_\omega^{E_r}(\mu)/J_\omega(\mu)}{J_\omega^{E_R}(\mu)/J_\omega(\mu)} = \frac{J_\omega^{E_r}(\mu)}{J_\omega^{E_R}(\mu)}$$

The jet shape is a ratio of 2 jet energy functions . The measured jet energy functions are obtained at 1 loop. We start from the natural scales that eliminate all large logarithms in the fixed order calculation and evolve to a common scale [resumming $\ln(r/R)$]

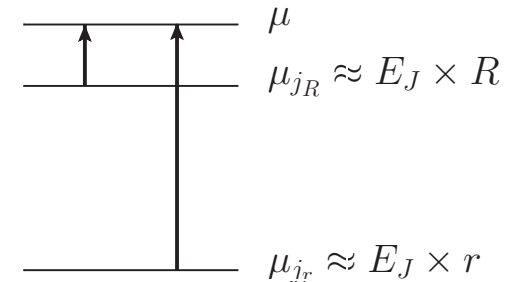
Result

Y.-T.Chien et al. (2014)

$$S(\nu, \mu) = - \int_{\alpha_s(\nu)}^{\alpha_s(\mu)} d\alpha \frac{\Gamma_{\text{cusp}}(\alpha)}{\beta(\alpha)} \int_{\alpha_s(\nu)}^{\alpha} \frac{d\alpha'}{\beta(\alpha')} ,$$

$$A_i(\nu, \mu) = - \int_{\alpha_s(\nu)}^{\alpha_s(\mu)} d\alpha \frac{\gamma^i(\alpha)}{\beta(\alpha)} , \quad A_\Gamma(\nu, \mu) = - \int_{\alpha_s(\nu)}^{\alpha_s(\mu)} d\alpha \frac{\Gamma_{\text{cusp}}(\alpha)}{\beta(\alpha)} ,$$

$$\Psi_\omega^i(r) = \frac{J_\omega^{iE_r}(\mu)}{J_\omega^{iE_R}(\mu)} = \frac{J_\omega^{iE_r}(\mu_{j_r})}{J_\omega^{iE_R}(\mu_{j_R})} \exp[-2C_i S(\mu_{j_r}, \mu_{j_R}) + 2A_i(\mu_{j_r}, \mu_{j_R})] \times \left(\frac{\mu_{j_r}^2}{\omega^2 \tan^2 \frac{R}{2}} \right)^{C_i A_\Gamma(\mu_{j_R}, \mu_{j_r})}$$



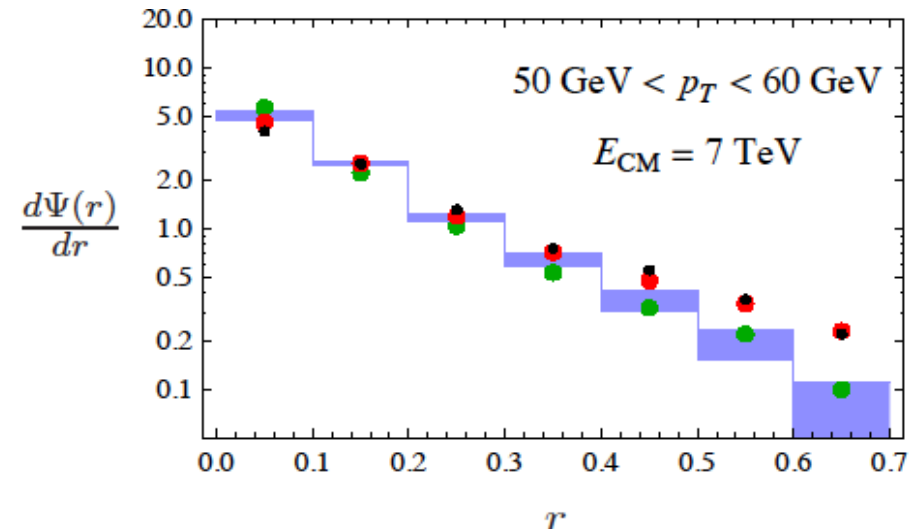
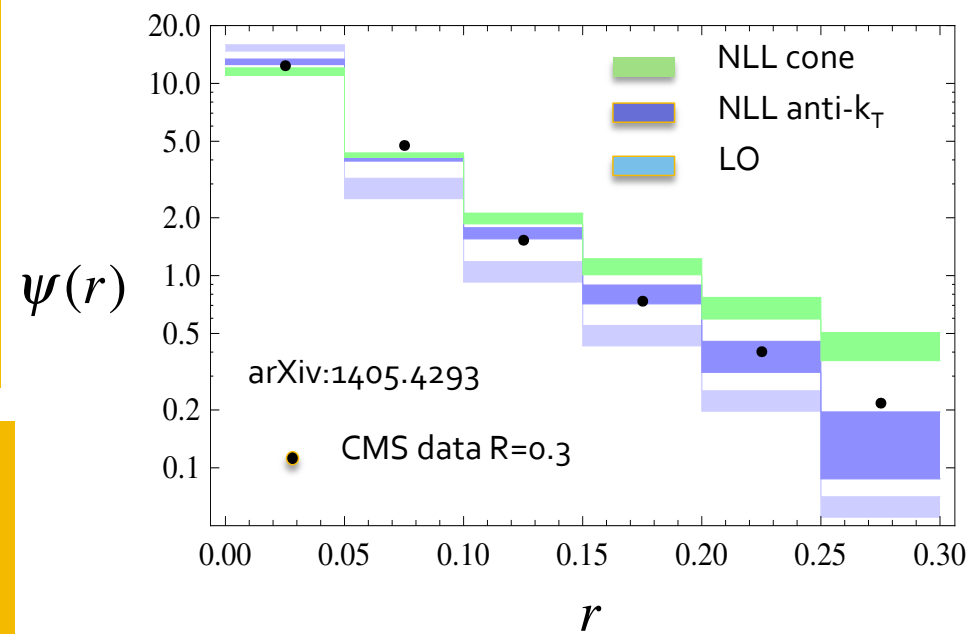
NLL results in p+p collisions

- We derived the algorithm dependence of the jet shapes (anti) k_T /cone
- Significant improvement over fixed order calculation

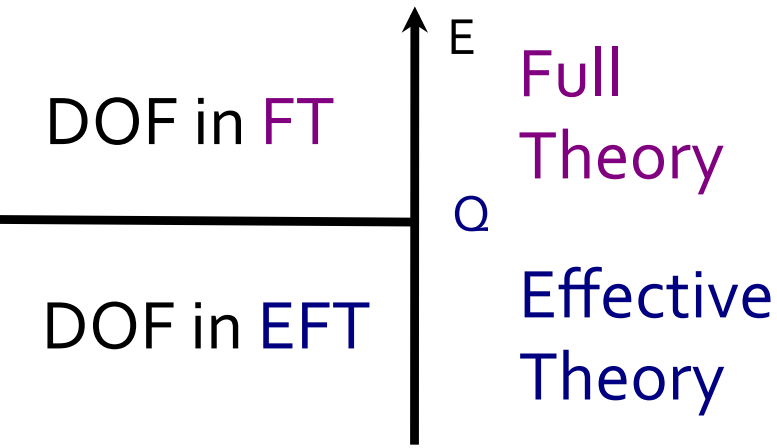
- The calculation does not include initial-state radiation/beam functions and hadronization effects
- Power suppressed but visible at the tail of the distribution and lower p_T

Y.-T.Chien et al. (2014)

See talk by Chien in this conference



Examples of effective field theories [EFTs]



- Simple but powerful idea to concentrate on the significant degrees of freedom [DOF].
Manifest power counting

| | Q | power counting | DOF in FT | DOF in EFT |
|--|------------------------|----------------------------|-----------|-------------------|
| Chiral Perturbation Theory (ChPT) | Λ_{QCD} | p/Λ_{QCD} | q, g | K, π |
| Heavy Quark Effective Theory (HQET) | m_b | Λ_{QCD}/m_b | Ψ, A | h_v, A_s |
| Soft Collinear Effective Theory (SCET) | Q | p_\perp/Q | Ψ, A | ξ_n, A_n, A_s |

III. In more detail: the jet scattering kinematics

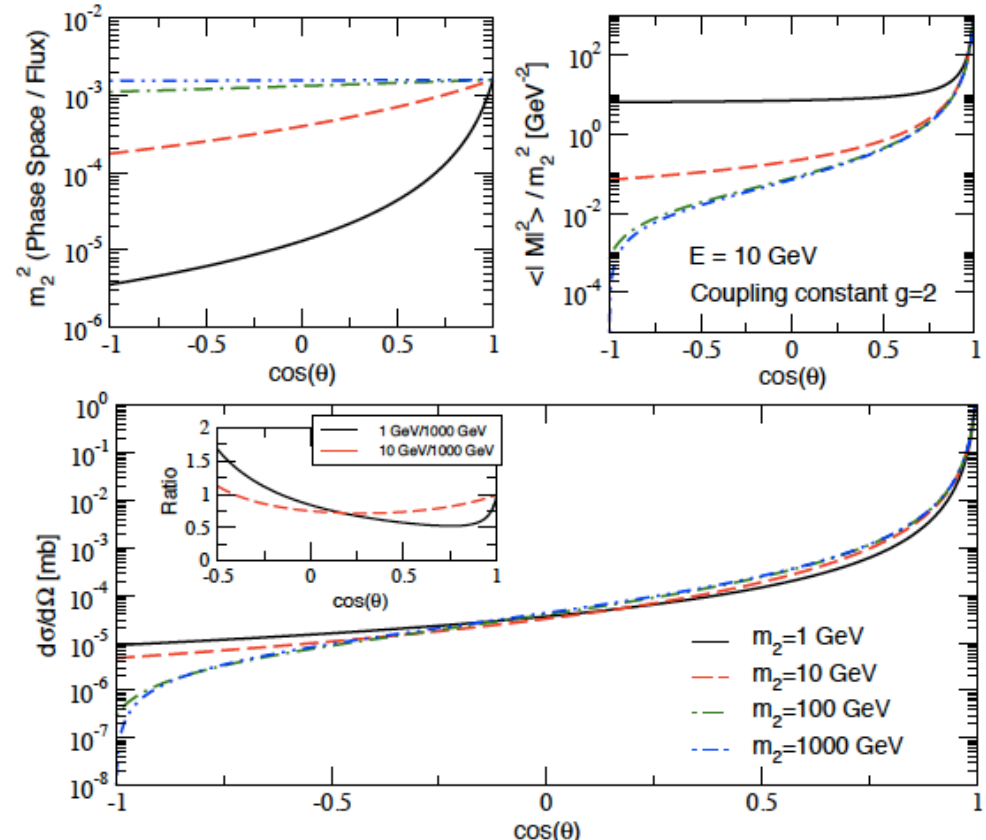
- What is missing in the YM Lagrangian is the interaction between the jet and the medium

- Kinematics and channels
 - t – jet broadening and energy loss
 - s – isotropisation
 - u – backward hard scattering

- Fully dynamic medium recoil, cross section reduction (5% – 15%). Completely dominated by forward scattering

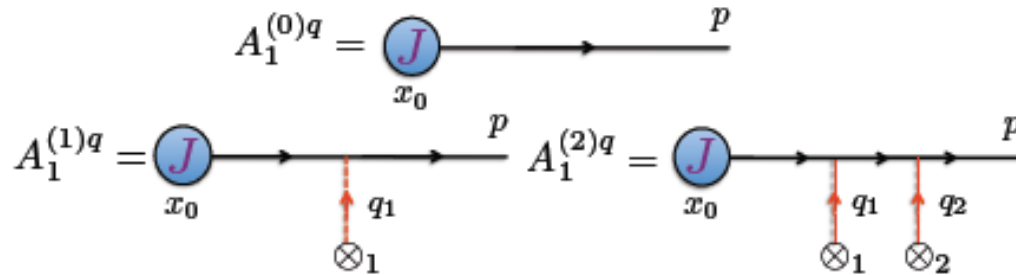
$$\frac{d\sigma}{d\Omega} \rightarrow \frac{d\sigma}{d^2\mathbf{q}_\perp} = \frac{C_2(R)C_2(T)}{d_A} \frac{|v(\mathbf{q}_\perp; E, m_1, m_2)|^2}{(2\pi)^2}$$

G. Ovanesyan et al. (2011)

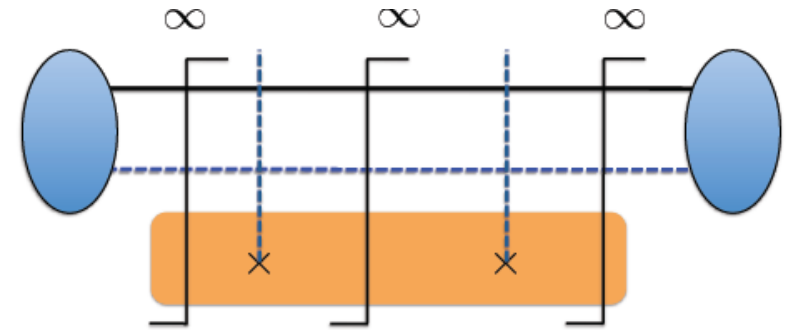


III. Main results: jet broadening

- Jet broadening and its gauge invariance



M. Gyulassy et al. (2001)



Classes of diagrams (single Born, double Born). Reaction Operator

- General result. Will evaluate the broadening (or lack off) of jets

$$\frac{dN^{(n)}(\mathbf{p}_\perp)}{d^2\mathbf{p}_\perp} = \prod_{i=1}^n \int_{z_{i-1}}^L \frac{dz_i}{\lambda} \int d^2\mathbf{q}_{\perp i} \left[\frac{1}{\sigma_{el}(z_i)} \frac{d\sigma_{el}(z_i)}{d^2\mathbf{q}_{\perp i}} \left(e^{-\mathbf{q}_{\perp i} \cdot \vec{\nabla}_{\mathbf{p}_\perp}} \right) - \delta^2(\mathbf{q}_\perp) \right] \frac{dN^{(0)}(\mathbf{p}_\perp)}{d^2\mathbf{p}_\perp}$$

- In special cases such as constant density and the Gaussian approximation

Starting with a collinear beam of quarks/gluons
we recover

M. Gyulassy et al. (2002)

$$\frac{dN(\mathbf{p}_\perp)}{d^2\mathbf{p}_\perp} = \frac{1}{2\pi} \frac{e^{-\frac{p^2}{2\chi\mu^2\xi}}}{\chi\mu^2\xi} \quad \chi = \frac{L}{\lambda}$$

III. Main results: in-medium splitting / parton energy loss

$$\frac{dN}{dx} \sim \left| \begin{array}{c} \text{Diagram 1} + \text{Diagram 2} + \text{Diagram 3} \\ \text{Diagram 4} + \text{Diagram 5} + \text{Diagram 6} \end{array} \right|^2 + 2\text{Re} \left[\begin{array}{c} \text{Diagram 7} + \text{Diagram 8} \\ \text{Diagram 9} + \text{Diagram 10} \end{array} \right] \times \text{Diagram 11}$$

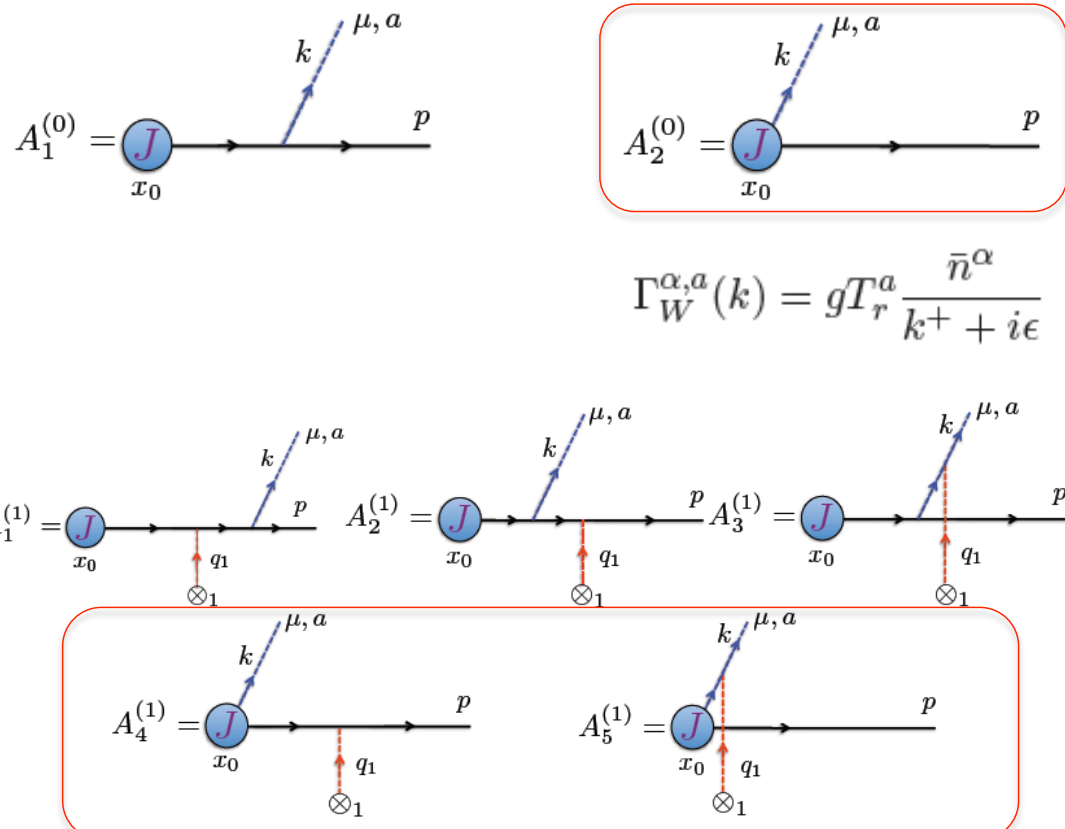
Gluon splitting functions factorize from the hard scattering cross section only for spin averaged processes

Altarelli-Parisi splitting

G. Altarelli et al. (1978)

- Note that a collinear Wilson line appears in the R_ξ gauge

Single Born diagrams



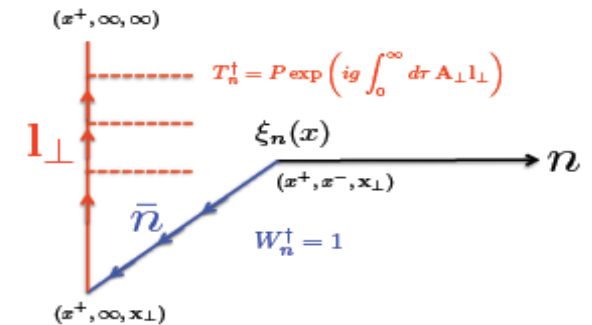
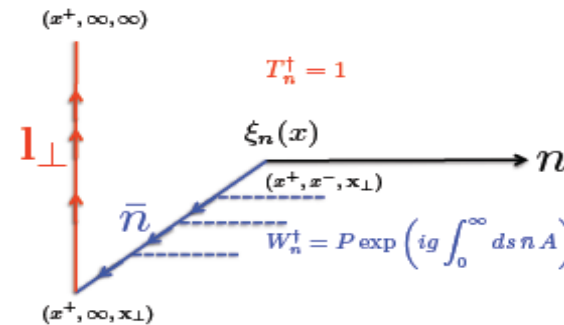
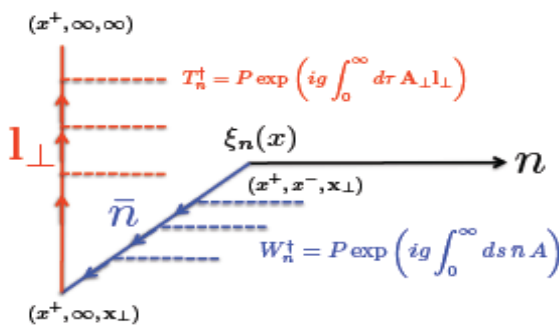
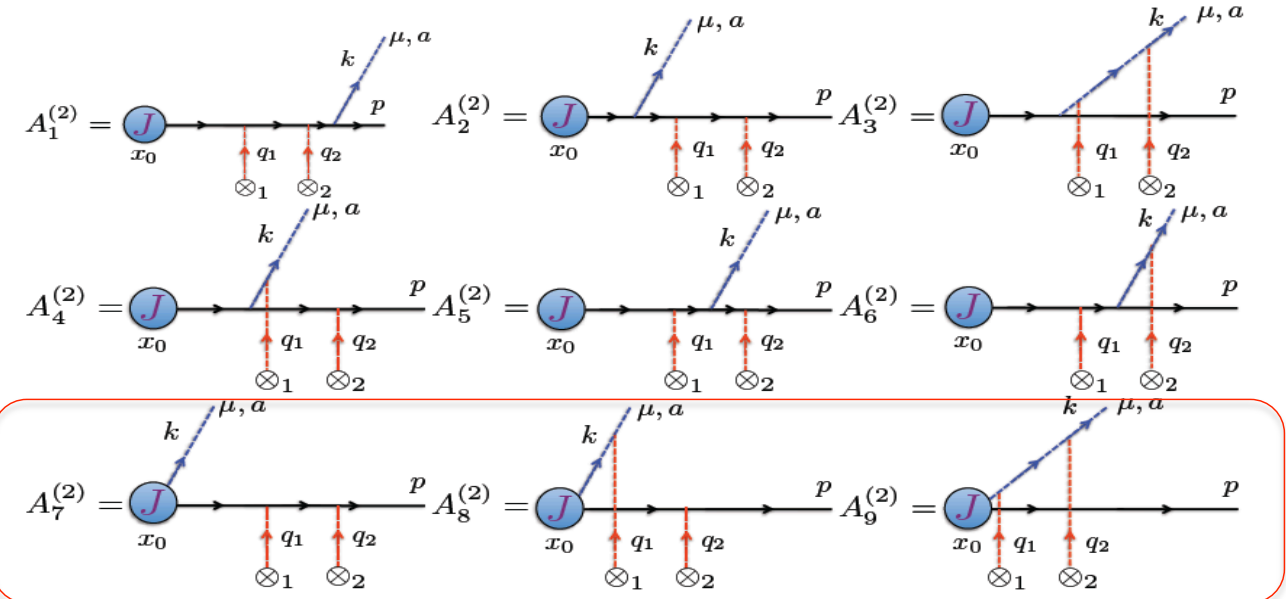
$$\Gamma_W^{\alpha,a}(k) = g T_r^a \frac{\bar{n}^\alpha}{k^+ + i\epsilon}$$

III. Main results: in-medium splitting / parton energy loss

Double Born diagrams

G. Ovanesyan et al. (2011)

- The lightcone gauge



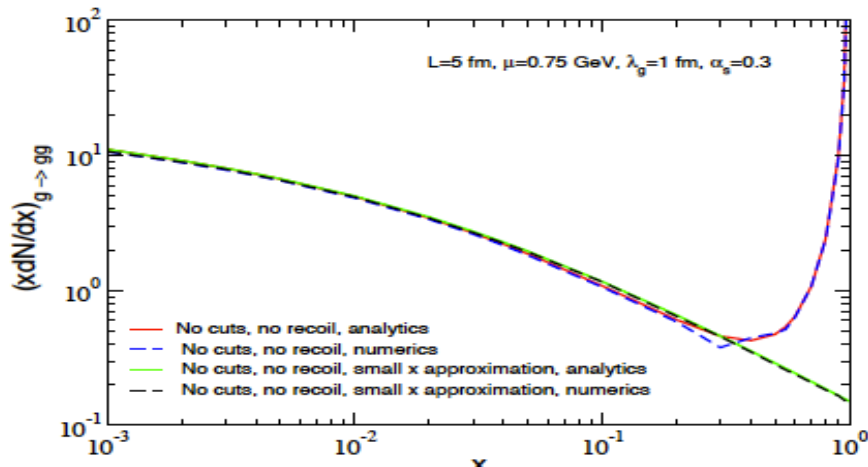
- New Feynman rule

$$A_\perp^{i,a} \otimes_{q} \mu, b = i \delta^{ab} \frac{\bar{n}^\mu q^i}{q^2 + i\varepsilon} C_\infty^{(\text{Pres})} \left(\frac{1}{q^+ + i\varepsilon} - \frac{1}{q^+ - i\varepsilon} \right)$$

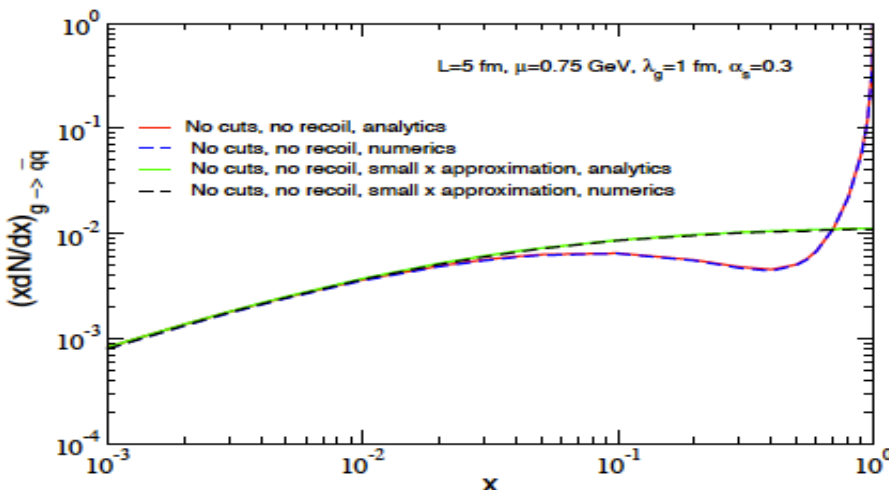
A. Idilbi et al. (2010)

III. Numerical examples

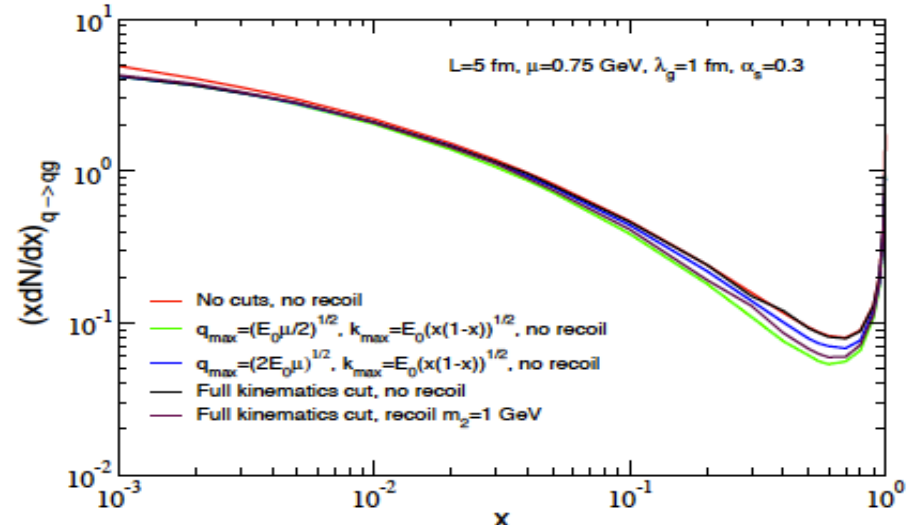
- Leading intensity term



- Sub-leading intensity term



- Kinematic effects

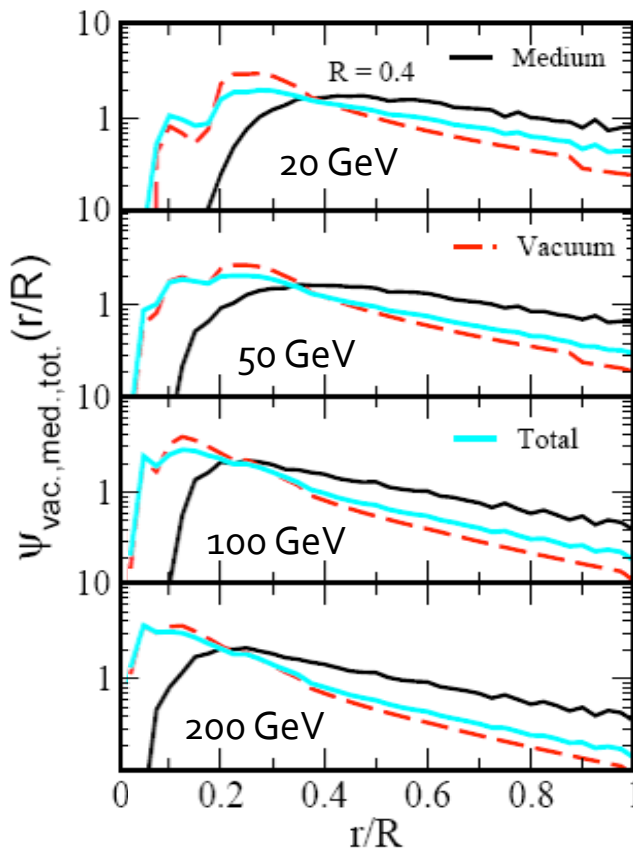


- We have theoretical control over the in-medium splittings
- The large- x and kinematic effects are of the same order
- Will be incorporated in future phenomenological applications

V. QGP – modified jet shapes

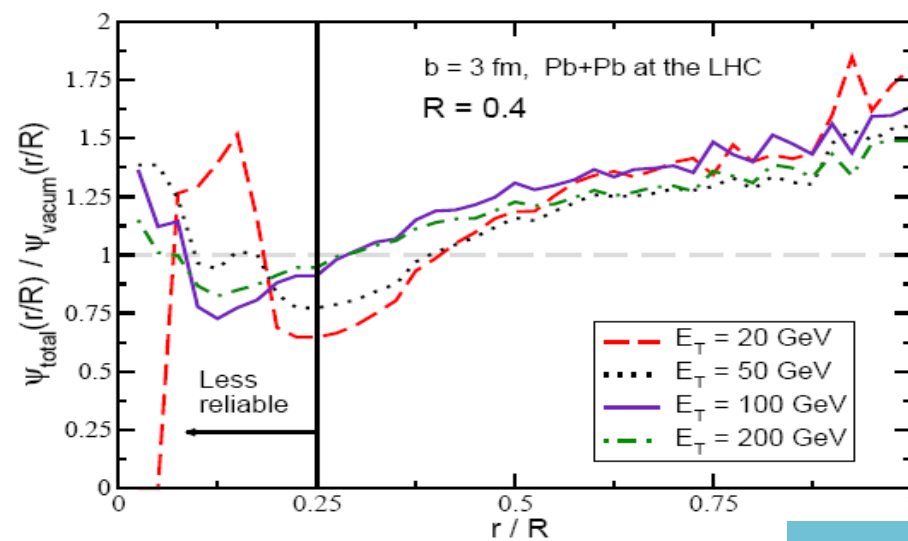
$$\Psi_{\text{int}}(r; R) = \frac{\sum_i (E_T)_i \Theta(r - (R_{\text{jet}})_i)}{\sum_i (E_T)_i \Theta(R - (R_{\text{jet}})_i)}$$

$$\psi(r; R) = \frac{d\Psi_{\text{int}}(r; R)}{dr}$$

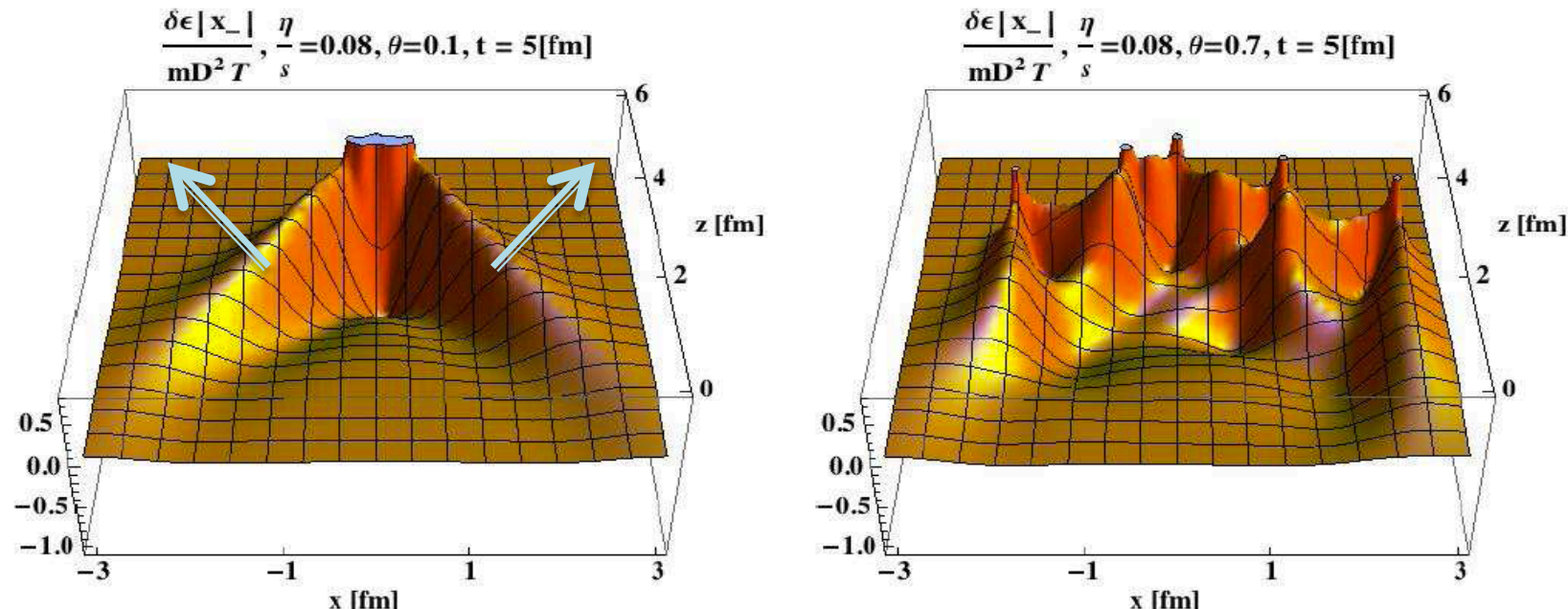


- Surprisingly, there is no big difference between the jet shape in vacuum and the total jet shape in the medium
- Take a ratio of the differential jet shapes

| R=0.4 | Vacuum | Complete E-loss | Realistic Case |
|------------------------------|--------|-----------------|----------------|
| <r/R>, $E_T = 20\text{GeV}$ | 0.41 | 0.57 | 0.45 |
| <r/R>, $E_T = 50\text{GeV}$ | 0.35 | 0.53 | 0.38 |
| <r/R>, $E_T = 100\text{GeV}$ | 0.28 | 0.42 | 0.32 |
| <r/R>, $E_T = 200\text{GeV}$ | 0.25 | 0.42 | 0.28 |



III. Why are Mach cones initiated by jets unlikely



- An individual parton (or a collinear system) can produce a Mach cone on an event by event basis. Multiple events will reduce the observable effect
- Typical medium-induced shower multiplicities are $N^g=4$ (quark) and $N^g=8$ (gluon) and emitted at large angles ~ 0.7 (much larger than in the vacuum)
- Each parton quickly becomes an individual source of excitation and these multiple sources wipe out any conical signature

I. Vitev (2005)

IV. Resummation, RG equations and Higgs production at the LHC

- SCET is very effective in resumming in large infrared logarithms using Renormalization group equations

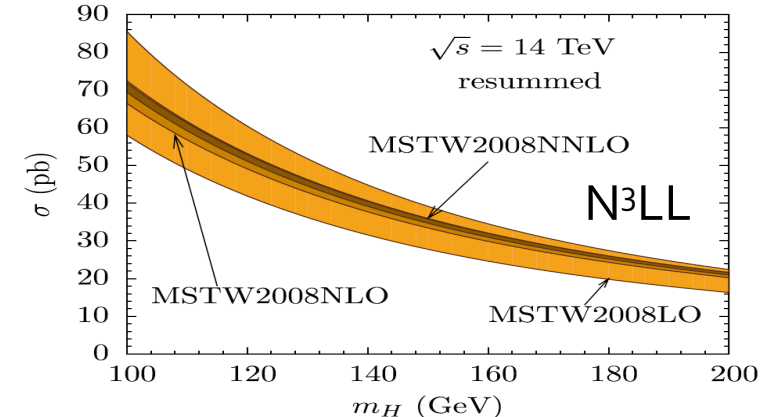
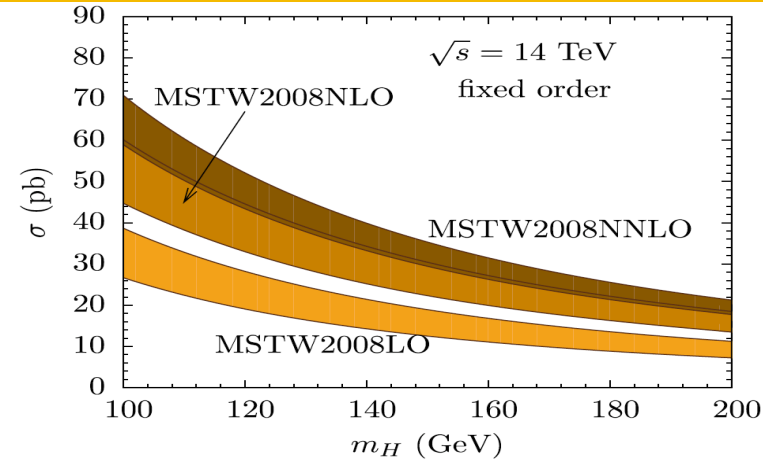
General structure of Sudakov logs

$$C(\bar{n} \cdot p, \mu) = 1 + a_s [L^2 + L + 1] + a_s^2 [L^4 + L^3 + L^2 + L + 1] + a_s^3 [L^6 + L^5 + L^4 + L^3 + L^2 + L + 1]$$

LL NLL

$$a_s = \frac{\alpha_s}{\pi}$$

$$L = \log \left(\frac{\mu}{\bar{n} \cdot p} \right)$$



- It can improve upon traditional techniques, such as CCS

IV. Factorization in SCET and angularities

- Factorization theorems have been proven in SCET for a number of observables: event shapes [e^+e^-], Higgs [pp], top [e^+e^-] ...
 - Angularity observables: generalization of traditional event shapes

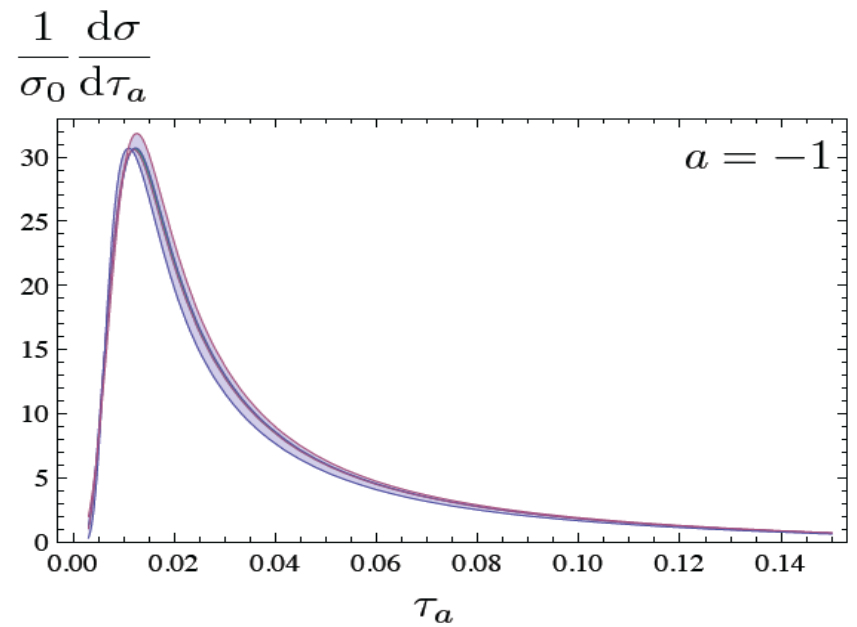
C. Berger et al. (2003)

$$\tau_a = \frac{1}{Q} \sum_i |\vec{p}_i^T| \exp(-\eta_i(1-a)) \quad -\infty < a < 2$$

- Factorized in hard function, jet functions and soft function

$$\frac{1}{\sigma_0} \frac{d\sigma}{de} = H(Q) \int de_n J_n(e_n) de_{\bar{n}} J_{\bar{n}}(e_{\bar{n}}) de_s S(e_s) \delta(e - e_n - e_{\bar{n}} - e_s)$$

C. Bauer et al. (2008)



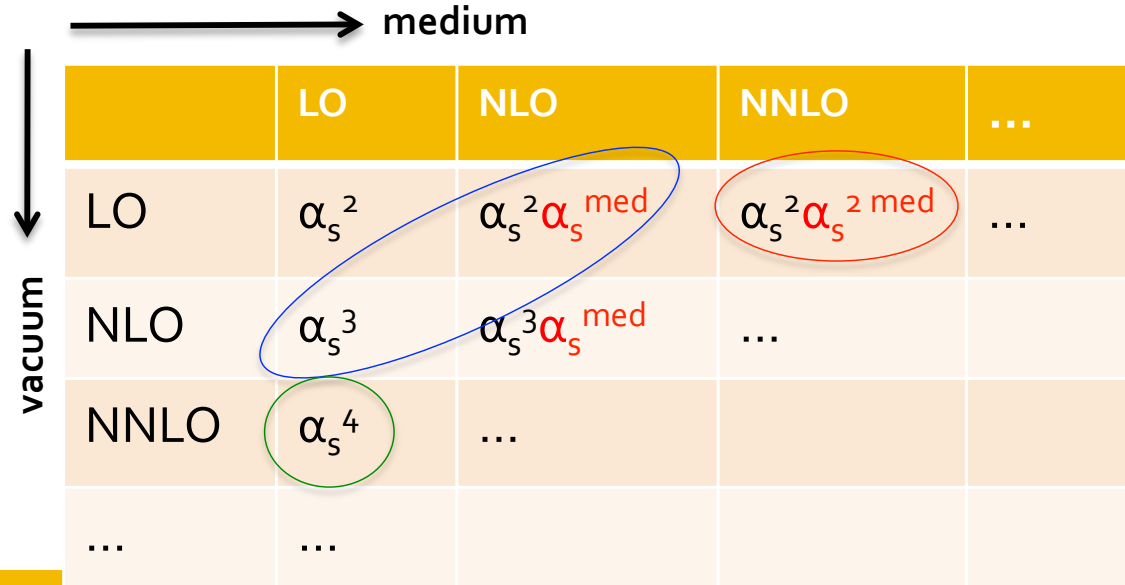
A. Hornig et al. (2010)

Splitting functions and the parton shower

- Making the connection to the standard LO, NLO, ...; LL, NLL ... pQCD approach (higher orders and resummation)

- Need to understand the process-dependent contributions

- Need to understand the dependence on the properties of the nuclear medium



- In the vacuum $O(\alpha_s^2)$ splitting kernels
- In the medium the full $O(\alpha_s)$ known , now being implemented
- In the medium $O(\alpha_s^2)$ only $q \rightarrow qgg$ known, computationally demanding

S. Catani et al. (1997)

G. Ovanesyan et al. (2011)

M. Fickinger et al. (2013)

SCET formulation

Energetic quarks and leptons
collinear modes

Include also soft quarks and gluons

C. Bauer et al. (2001)

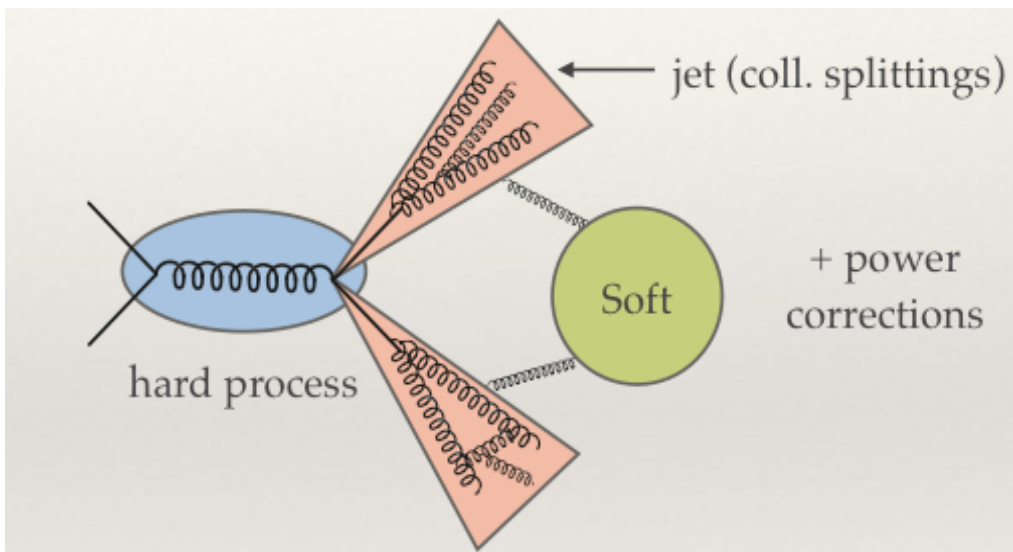
D. Pirol et al. (2004)

$$p_c = (p_+, p_-, p_\perp) \sim \left(\frac{\Lambda^2}{Q}, Q, \Lambda \right) = Q(\lambda^2, 1, \lambda)$$

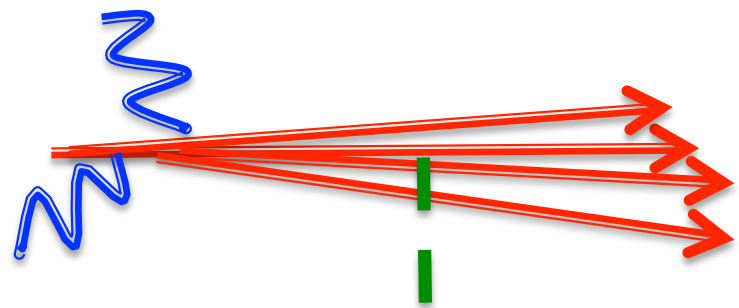
$$p_s = (p_+, p_-, p_\perp) \sim (\Lambda, \Lambda, \Lambda) = Q(\lambda, \lambda, \lambda)$$

- SCET Lagrangian to all orders in λ [Can expand to LO, NLO,...]

| | |
|-------------------------------|----------------------|
| Collinear quarks, antiquarks | $\xi_n, \bar{\xi}_n$ |
| Collinear gluons, soft gluons | A_n, A_s |



- The missing mode



$$q \sim [\lambda^2, \lambda^2, \lambda]$$

A new mode – the Glauber gluon

The vacuum splitting kernels

- In the vacuum we have the DGPAL splitting kernels that factorize from the hard scattering cross section and are process independent

Gribov et al. (1972)

G. Altarelli et al. (1977)

Y. Dokshitzer (1977)

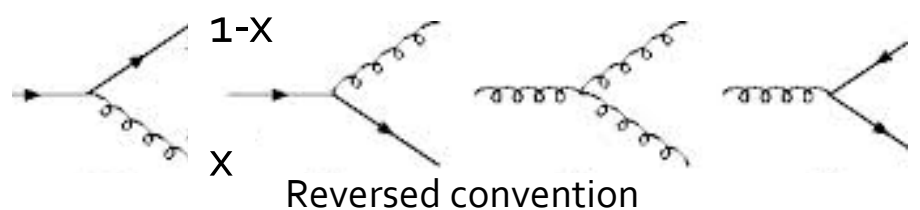
- The singular pieces A, B can be obtained from flavor and momentum conservation sum rules
- Can be re-derived using SCET. Use only the collinear sector

$$\left(\frac{dN}{dx d^2\mathbf{k}_\perp} \right)_{q \rightarrow qg} = \frac{\alpha_s}{2\pi^2} C_F \frac{1 + (1-x)^2}{x} \frac{1}{\mathbf{k}_\perp^2}, \quad (\dots l_+ + A\delta(x))$$

$$\begin{aligned} \left(\frac{dN}{dx d^2\mathbf{k}_\perp} \right)_{g \rightarrow gg} &= \frac{\alpha_s}{2\pi^2} 2C_A \left(\frac{1-x}{x} + \frac{x}{1-x} \right. \\ &\quad \left. + x(1-x) \right) \frac{1}{\mathbf{k}_\perp^2}, \quad (\dots l_+ + B\delta(x)) \end{aligned}$$

$$\left(\frac{dN}{dx d^2\mathbf{k}_\perp} \right)_{g \rightarrow q\bar{q}} = \frac{\alpha_s}{2\pi^2} T_R \ (x^2 + (1-x)^2) \frac{1}{\mathbf{k}_\perp^2}$$

$$\left(\frac{dN}{dx d^2\mathbf{k}_\perp} \right)_{q \rightarrow gq} = \left(\frac{dN}{dx d^2\mathbf{k}_\perp} \right)_{q \rightarrow qg} (x \rightarrow 1-x)$$



$$\int_0^1 P_{qq}(x) dx = 0,$$

$$\int_0^1 [P_{qq}(x) + P_{gq}(x)] (1-x) dx = 0,$$

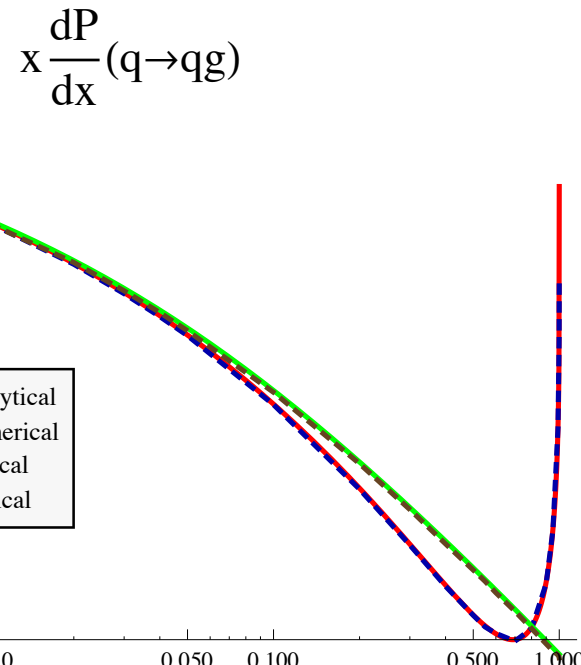
$$\int_0^1 [2n_f P_{gq}(x) + P_{gg}(x)] (1-x) dx = 0.$$

The soft-gluon energy loss limit

Take the small- x soft gluon emission limit

$$x \left(\frac{dN}{dx} \right) \left\{ \begin{array}{l} q \rightarrow qg \\ g \rightarrow gg \end{array} \right\} = \frac{\alpha_s}{\pi^2} \left\{ \begin{array}{l} C_F[1 + \mathcal{O}(x)] \\ C_A[1 + \mathcal{O}(x)] \end{array} \right\} \int \frac{d\Delta z}{\lambda_g(z)} \int d^2\mathbf{k}_\perp d^2\mathbf{q}_\perp \frac{1}{\sigma_{el}} \frac{d\sigma_{el}^{\text{medium}}}{d^2\mathbf{q}_\perp}$$
$$\times \frac{2\mathbf{k}_\perp \cdot \mathbf{q}_\perp}{\mathbf{k}_\perp^2 (\mathbf{k}_\perp - \mathbf{q}_\perp)^2} \left[1 - \cos \frac{(\mathbf{k}_\perp - \mathbf{q}_\perp)^2}{xp_0^+} \Delta z \right].$$

M Gyulassy et al . (2000)



The result reduces to the GLV energy-loss differential intensities

- Only 2 medium-induced splittings survive
- There is no flavor mixing
- Results can be interpreted as energy loss

Medium-modified evolution of the fragmentation functions

- Using the same techniques. The vacuum and the medium induced evolution factorize

$$\frac{d \ln D_{h/c}^{\text{med.}}(z, Q)}{d \ln Q} = [\dots]_{\text{vac.}} - [n(z) - 1] \left\{ \int_0^{1-z} dz' z' Q \frac{dN}{dz' dQ}(z', Q) \right\} - \int_{1-z}^1 dz' Q \frac{dN}{dz' dQ}(z', Q) .$$

$$D_{h/c}^{\text{med.}}(z, Q) = e^{-2C_R \frac{\alpha_s}{\pi} \left[\ln \frac{Q}{Q_0} \right] \{ [n(z) - 1](1-z) - \ln(1-z) \}} D_{h/c}(z, Q_0)$$

$$\times e^{-[n(z)-1] \left\{ \int_0^{1-z} dz' z' \int_{Q_0}^Q dQ' \frac{dN}{dz' dQ'}(z', Q') \right\} - \int_{1-z}^1 dz' \int_{Q_0}^Q dQ' \frac{dN}{dz' dQ'}(z', Q')}$$

$$= D_{h/c}(z, Q) e^{-[n(z)-1] \left\langle \frac{\Delta \tilde{E}}{E} \right\rangle_z - \langle N^g \rangle_z} .$$

- The main result:* direct relation between the evolution and energy loss approaches first established here

$$\left\langle \frac{\Delta \tilde{E}}{E} \right\rangle_z = \int_0^{1-z} dz' z' \int_{Q_0}^Q dQ' \frac{dN}{dz' dQ'}(z', Q') = \int_0^{1-z} dz' z' \frac{dN}{dz'}(z') \quad \rightarrow_{z \rightarrow 0} \left\langle \frac{\Delta E}{E} \right\rangle ,$$

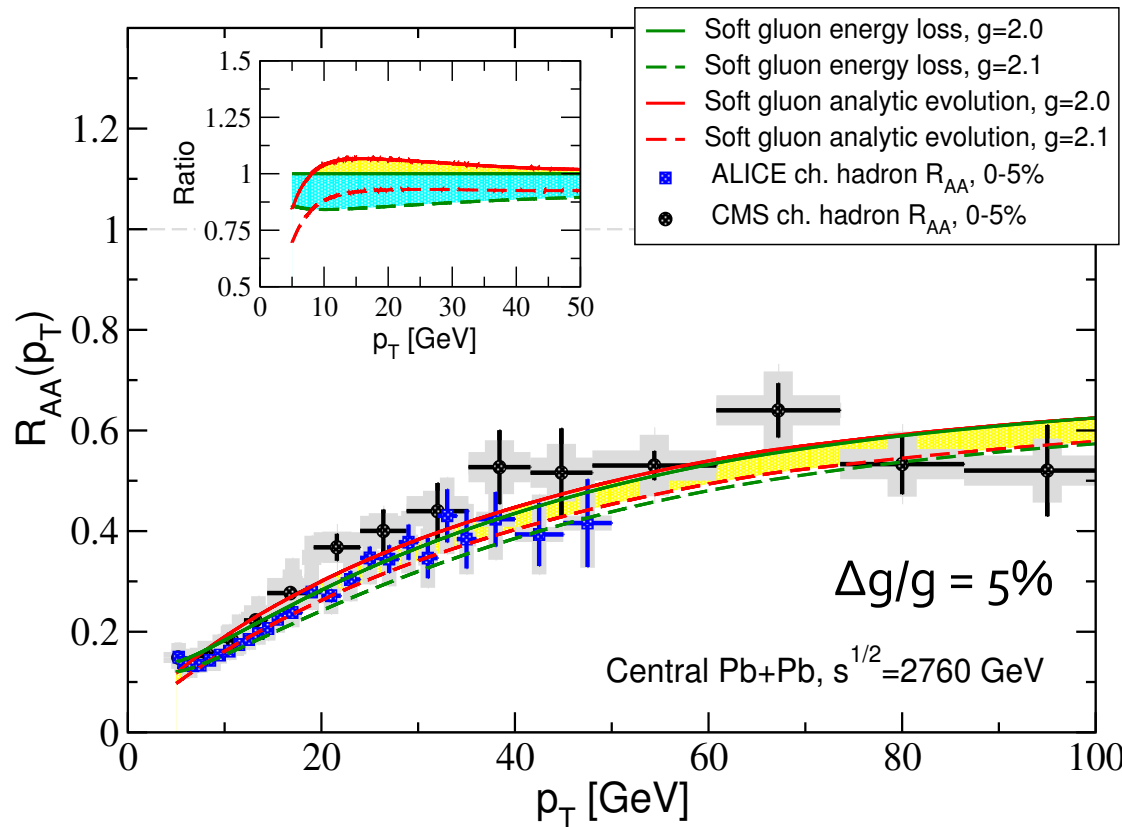
$$\langle N^g \rangle_z = \int_{1-z}^1 dz' \int_{Q_0}^Q dQ' \frac{dN}{dz' dQ'}(z', Q') = \int_{1-z}^1 dz' \frac{dN}{dz'}(z') \quad \rightarrow_{z \rightarrow 1} \langle N^g \rangle .$$

G. Ovanesyan et al. (2014)

Numerical results: E-loss vs analytic evolution in the soft gluon limit

■ The energy loss approach

Note that we have ignored other nuclear matter effects: Cronin effect, cold nuclear matter energy loss, power corrections/shadowing. At the LHC final-state effects dominate

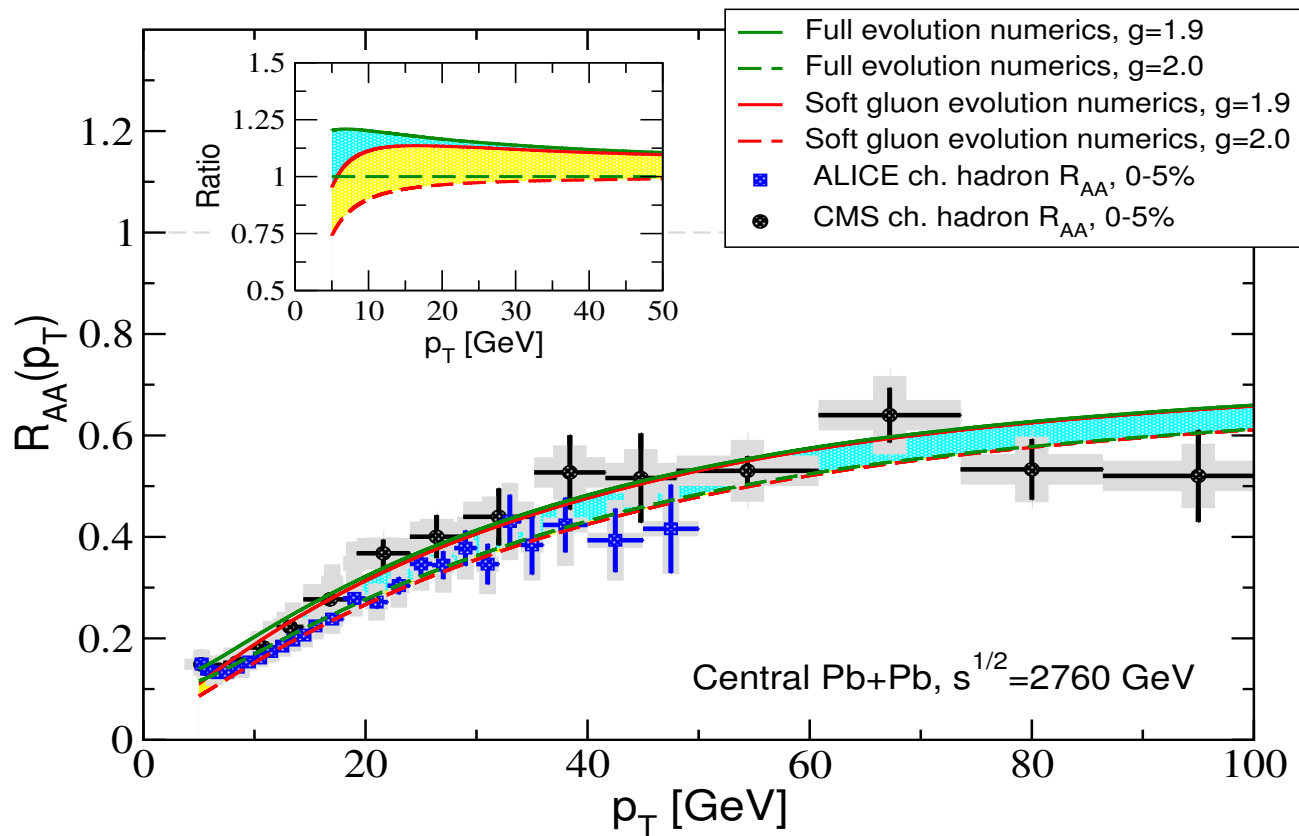


MC code was written by our summer visitor to evaluate the e-loss/medium splittings

The coupling between the jet and the medium can be constrained to 5%, The scattering cross sections/ properties of the medium to 20% ($\sim g^4$)

Numerical results: full-x vs small-x evolution

- Implement the fully numerical solution of the DGLAP evolution equations

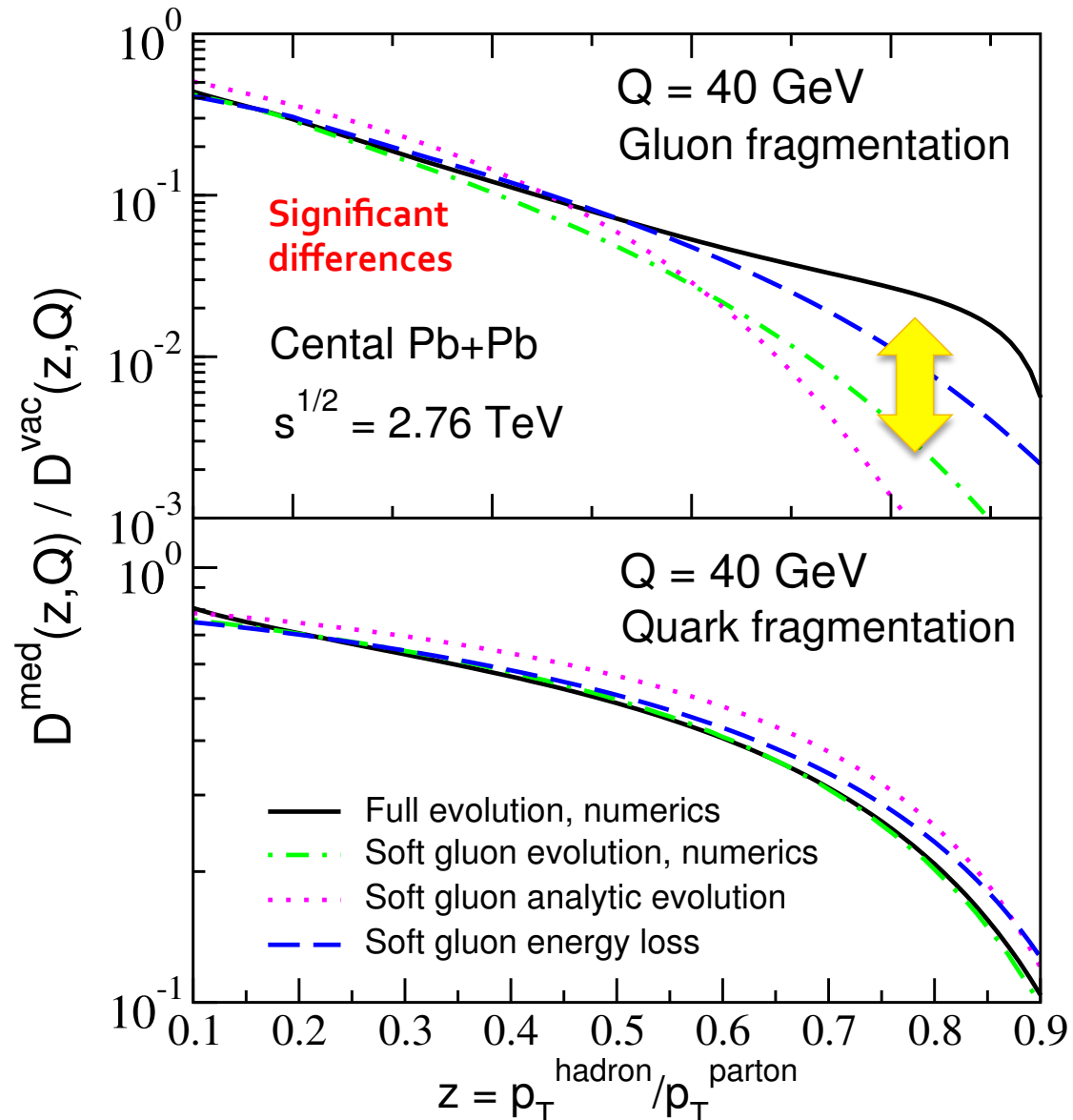


- The coupling between the jet and the medium can be constrained to the same accuracy - 5%

Future directions

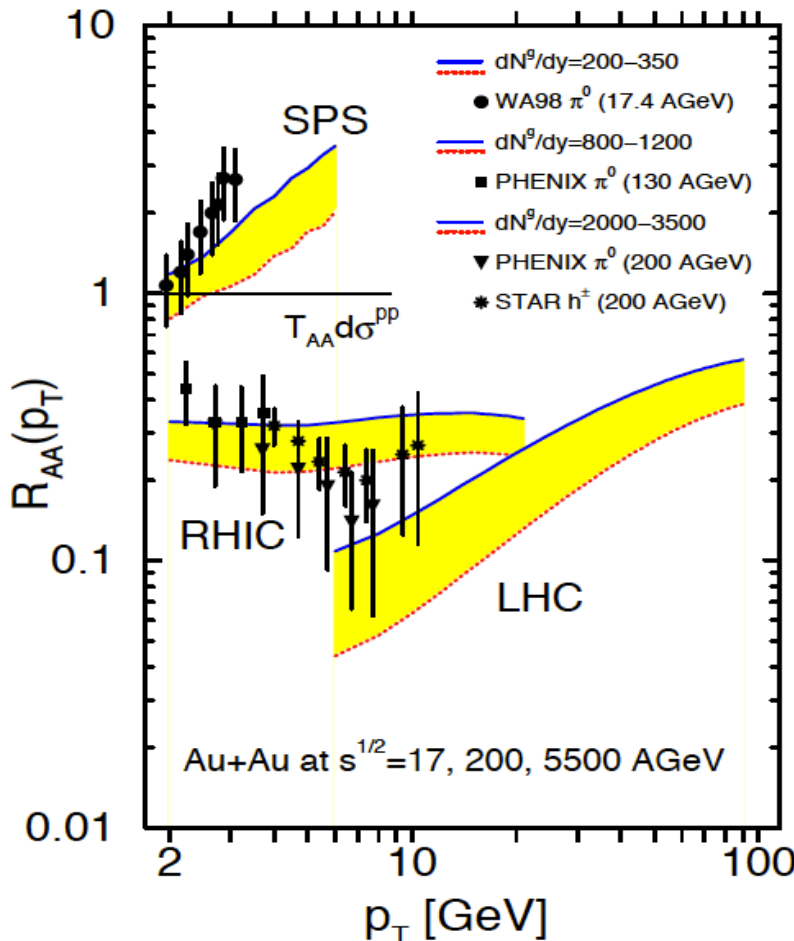
“Modified” fragmentation functions

- Dominated by quark fragmentation, small differences, inclusive measurements
- Points the directions where significant improvement can be expected – longitudinal and transverse structure of jets, tagged jets and dijets



Traditional E-loss – successful but open questions remain

- While still LO, it predicted in 2002, 2006 – the R_{AA} at high p_T for both RHIC and LHC

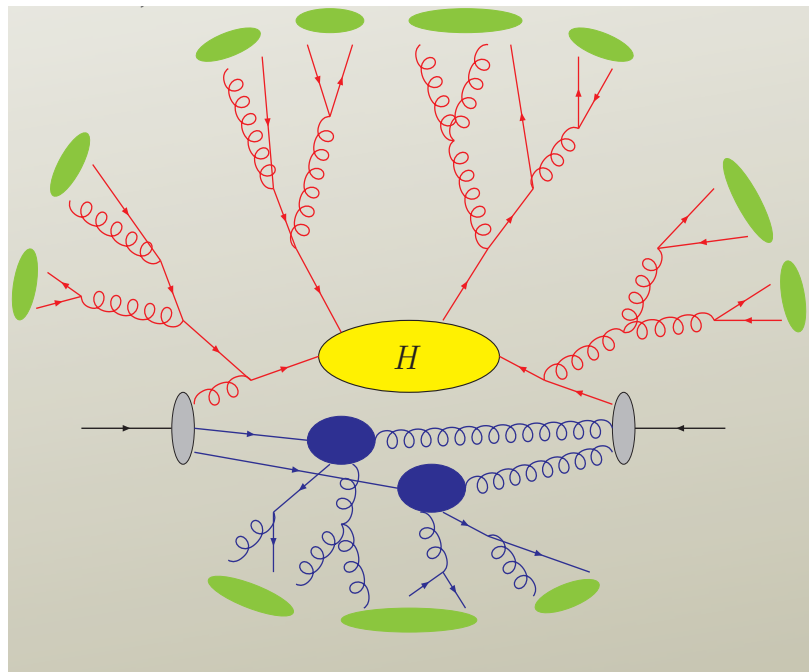


Include the quenched parton and the radiative gluon fragmentation

- Difficult to make connection to the standard LO, NLO, ...; LL, NLL ... pQCD approach (higher orders and resummation)
- There is considerable model dependence and it is difficult to systematically improve this approach

I. V., M. Gyulassy (2002)

Evolution and resummation of large logarithms



Gribov et al. (1972)

$$\frac{dD_{h/q}(z, Q)}{d \ln Q} = \frac{\alpha_s(Q)}{\pi} \int_z^1 \frac{dz'}{z'} \left[P_{q \rightarrow qg}(z') D_{h/q}\left(\frac{z}{z'}, Q\right) + P_{q \rightarrow gg}(z') D_{h/g}\left(\frac{z}{z'}, Q\right) \right]$$

$$\frac{dD_{h/g}(z, Q)}{d \ln Q} = \frac{\alpha_s(Q)}{\pi} \int_z^1 \frac{dz'}{z'} \left[P_{g \rightarrow gg}(z') D_{h/g}\left(\frac{z}{z'}, Q\right) + P_{g \rightarrow q\bar{q}}(z') \sum_q D_{h/q}\left(\frac{z}{z'}, Q\right) \right]$$

- Collinear splitting kernels

$$\left(\frac{dN}{dx d^2 k_\perp} \right)_{q \rightarrow qg} = \frac{\alpha_s}{2\pi^2} C_F \frac{1 + (1-x)^2}{x} \frac{1}{k_\perp^2} \equiv \frac{\alpha_s}{2\pi^2} \frac{1}{k_\perp^2} P_{qg}^{\text{real}}(x),$$

$$P_{gg}^{\text{real}}(x) = 2C_A \left(\frac{1-x}{x} + \frac{x}{1-x} + x(1-x) \right)$$

$$P_{gq}^{\text{real}}(x) = T_R (x^2 + (1-x)^2),$$

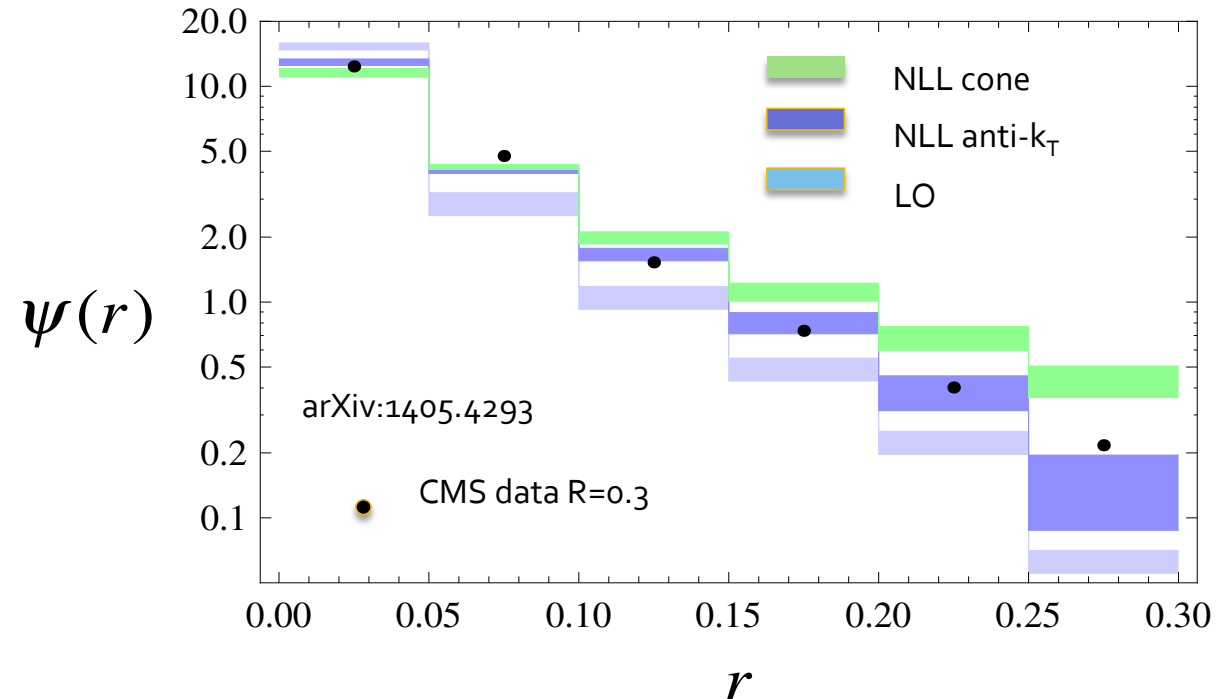
$$P_{qq}^{\text{real}}(x) = C_F \frac{1+x^2}{1-x}.$$

G. Altarelli et al. (1977)

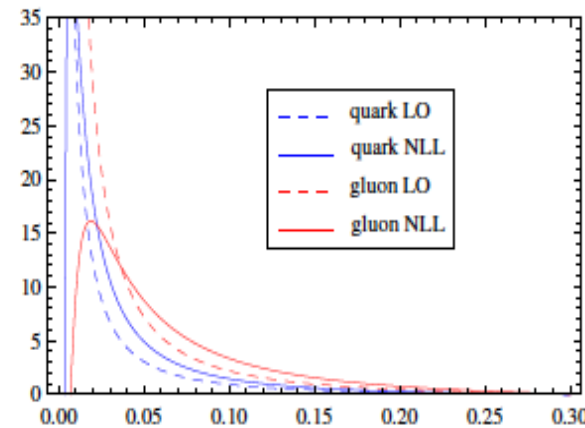
- Yield LLA or MLLA (LL')

Numerical NLL results in p+p collisions

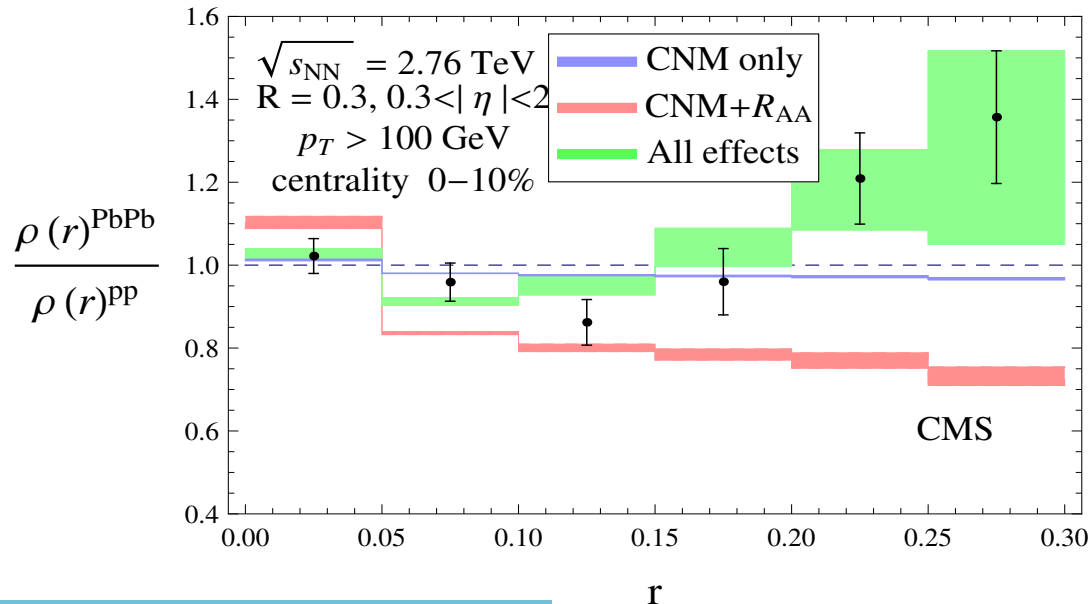
- We derived the algorithm dependence of the jet shapes (anti) k_T vs cone
- Significant improvement over fixed order calculation
- For large radii (0.7) works less well (hadronization et al.) also for smaller energies



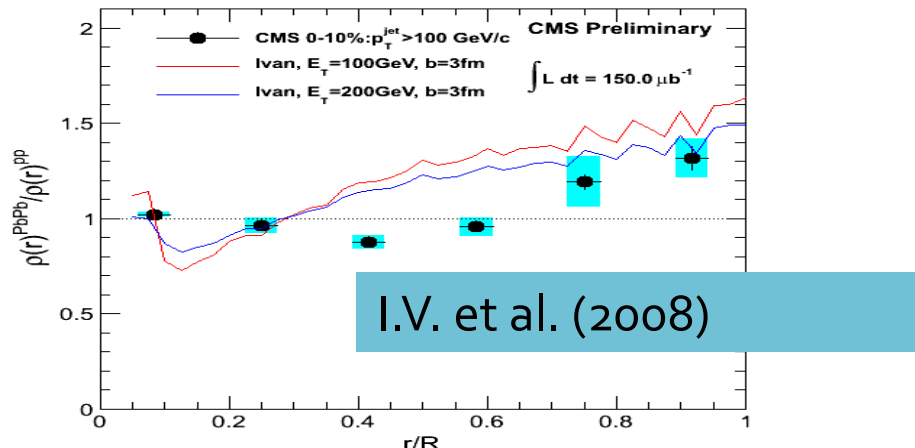
Just to show that
the fixed order is
divergent



Jet shape modification in heavy ion collisions



Y.-T. Chien et al. (2015)



I.V. et al. (2008)

- Improvements relative to the traditional E-loss approach are indeed significant
- CNM effects do not play a role in intrajet (or jet correlation observables)
- Jet quenching alone leads to narrowing of the shape.
- The broad parton shower leads to enhancement in the periphery